

## Effects of the on-site Coulomb repulsion in double-exchange magnets

D. I. Golosov\*

*Department of Condensed Matter Physics, Weizmann Institute of Science, Rehovot 76100, Israel  
and Theoretical Physics, Oxford University, 1 Keble Rd., Oxford OX1 3NP, United Kingdom*

(Received 18 June 2004; published 21 January 2005)

We investigate the zero-temperature phase diagram and spin-wave properties of a double exchange magnet with on-site Hubbard repulsion. It is shown that even within a simple Hartree-Fock approach this interaction (which is often omitted in theoretical treatments) leads to qualitatively important effects which are highly relevant in the context of experimental data for the colossal magnetoresistance compounds. These include the asymmetry of the doping dependence of spin stiffness, and the zone-boundary “softening” of spin wave dispersion. Effects of Hubbard repulsion on phase separation are analyzed as well. We also show that in the ferromagnetic phase, an unusual temperature-dependent effective electron-electron interaction arises at finite  $T$ . The mean-field scheme, however, does not yield the experimentally observed density of states depletion near the Fermi level. We speculate that the proper treatment of electron-electron interactions may be necessary for understanding both this important feature and more generally the physics of colossal magnetoresistance phenomenon.

DOI: 10.1103/PhysRevB.71.014428

PACS number(s): 75.47.Gk, 75.47.Lx, 75.30.Ds, 75.10.Lp

### I. INTRODUCTION

The phenomenon of colossal magnetoresistance (CMR) is known to occur in a broad group of compounds, corresponding to different crystal structures, chemical compositions, and doping levels.<sup>1</sup> In addition to various heavily doped manganese oxides, the CMR effect is also observed in certain magnetic semiconductors and spinels;<sup>2</sup> it is natural to expect that in all these cases, the physical origins of the CMR are similar. Thus, a proper minimal theoretical model of a CMR system should account for the important common features shared by all these materials, while leaving out the peculiarities of crystal environment and atomic structure of individual compounds. It is universally recognized that one of these common features is the sizable ferromagnetic Hund’s rule coupling,  $J_H$ , between the spins of magnetic ions and those of conduction electrons, which gives rise to the double exchange ferromagnetism<sup>3</sup> of the CMR compounds. The purpose of the present article is to draw attention to the fact that another ubiquitous intra-atomic interaction, namely the Coulomb (Hubbard) repulsion  $U$ , also affects magnetic, electronic, and transport properties of the system in a profound way, and may play a crucial role in the basic physics of the CMR. While some effects of this interaction have been addressed in the past (see, e.g., Refs. 4–7), its potential importance is not yet fully appreciated. We will argue that the on-site Coulomb repulsion strongly affects the magnetic properties of the system; some generic experimental facts are recovered. We also suggest that the effects of Hubbard repulsion merit further investigation beyond the mean-field approach.

We start with the standard double exchange Hamiltonian, supplemented with a Hubbard repulsion term:

$$\mathcal{H} = -\frac{t}{2} \sum_{(i,j),\alpha} (c_{i\alpha}^\dagger c_{j\alpha} + c_{j\alpha}^\dagger c_{i\alpha}) - \frac{J_H}{2S} \sum_{i,\alpha,\beta} \vec{S}_i \vec{\sigma}^{\alpha\beta} c_{i\alpha}^\dagger c_{i\beta} + \frac{J}{S^2} \sum_{(i,j)} \vec{S}_i \vec{S}_j + U \sum_i c_{i\uparrow}^\dagger c_{i\downarrow}^\dagger c_{i\downarrow} c_{i\uparrow}. \quad (1)$$

Here, the fermionic operators  $c_{j\alpha}$  correspond to conduction electrons, hopping between the atomic sites of magnetic ions with spins  $\vec{S}_i$ , and the vector  $\vec{\sigma}^{\alpha\beta}$  is composed of Pauli matrices. Electron concentration is denoted by  $x$ , hence the hole density is given by  $1-x$  (we note that in the experimental literature on the CMR manganates, the opposite convention is often used). In order to discuss our results within the context of experimentally observed magnetic phase diagrams of the CMR manganates, we also include the antiferromagnetic superexchange coupling  $J$  between the ionic spins. We will treat the ionic spins as classical,  $S \gg 1$ ; quantum corrections are not expected to modify the effects of Hubbard term in a qualitative way. For the case of CMR manganates,  $S = 3/2$ , and the band theory calculations<sup>5,8</sup> suggest the typical values of  $t \sim 0.3-0.5$  eV,  $J_H \sim 2.5$  eV, and  $U \sim 8$  eV. The value of  $J$  can be roughly estimated from the experimentally observed Néel temperatures in the fully doped (no conduction  $e_g$  electrons,  $x=0$ ) case,<sup>9-11</sup>  $T_N \sim 100-200$  K, yielding  $J \sim 5-10$  meV. We will consider the case of a square (2D) or simple cubic (3D) lattice, assuming that the lattice spacing is equal to unity. Throughout the paper, chemical potential is denoted by  $\mu - (J_H/2)$ .

While the important and highly nontrivial effects of the orbital degree of freedom in the CMR manganates are of great interest to both theorists and experimentalists working in the field,<sup>1</sup> in writing Eq. (1) we assumed that there is only one atomic orbital available to conduction electrons at each site. The reasons for this drastic simplification are three-fold: (i) in the CMR manganates, orbital structure is strongly dependent on the crystalline environment and varies for different compounds and doping levels;<sup>12</sup> (ii) yet another situation takes place for magnetic semiconductors exhibiting CMR, like EuS or EuSe, where the three  $t_{2g}$  conduction bands show no Jahn-Teller splitting; therefore at present it seems difficult to conclude that a realistic treatment of orbital effects is crucial for understanding the basic physics of the CMR phenomenon; and (iii) we will see that the effects of Hubbard

repulsion are rather complex already in the single-orbital case; we believe that these should be understood before a more complicated model<sup>6</sup> is advanced.

We begin with a brief overview of the low-temperature properties of the double exchange model, Eq. (1) with  $U=0$ . The carrier spectrum in the ferromagnetic state of a 2D (3D) system is given by  $\epsilon_k^{\uparrow,\downarrow} = \mp (J_H/2) + \epsilon_{\vec{k}}$  with  $\epsilon_{\vec{k}} = -t \cos k_x - t \cos k_y (-t \cos k_z)$ . A sufficiently large value of Hund's rule coupling  $J_H$  then results in a complete spin polarization (*half-metal*) of conduction electrons within the entire doping range of  $0 < x \leq 1$ , in agreement with experimental data<sup>13</sup> (see, however, Ref. 14). At  $J_H \rightarrow \infty$  and  $J=0$ , any deviation of ionic spins from ferromagnetic order results, via the double exchange mechanism,<sup>3</sup> in a narrowing of the spin-up conduction band, and therefore costs positive energy. The corresponding value of spin stiffness  $D$  is then proportional to conduction band energy,  $DS = |E|/4d$  with  $E = \int \epsilon_{\vec{k}} n_{\vec{k}} d^d k / (2\pi)^d$  (where  $n_{\vec{k}}$  is the Fermi distribution function and  $d$  is the dimensionality of the system) and is therefore symmetric in electron density  $x$  with respect to the quarter-filling,  $x=1/2$ . In a more general case of finite  $J_H$  and  $J > 0$ , this *double exchange ferromagnetism* competes against antiferromagnetic tendencies, which originate from two distinct physical sources. In addition to the direct superexchange contribution  $J$  (which is responsible for the antiferromagnetism of the system at  $x=0$  and, roughly, can be assumed to be doping-independent), there arises an *indirect* antiferromagnetic interaction<sup>15</sup> which further lowers the relative energy of antiferromagnetic phases. This interaction is due to virtual transitions of conduction electrons between the two components of the spin-split band,<sup>16</sup> and its strength increases with increasing electron density  $x$ . Indeed, the net antiferromagnetic contribution to the spin stiffness  $DS$  of a double exchange ferromagnet at  $x \ll 1$  equals  $-J - \pi x^2 t^2 / (2J_H)$  in 2D and  $-J - (6\pi)^{2/3} x^{5/3} t^2 / (10J_H)$  in 3D, and grows to  $-J - t^2 / (4J_H)$  at  $x=1$ . While the actual destabilization of the ferromagnetic phase with increasing strength of antiferromagnetism proceeds via phase separation,<sup>2,17,18</sup> rather than a spin-wave mediated phase transition, this behavior of spin stiffness is in line with the overall conclusion on the phase diagram asymmetry: *in the  $U=0$  case, antiferromagnetic tendencies are more pronounced at  $x > 1/2$  than at  $x < 1/2$ .*

This expected behavior does not agree<sup>4</sup> with the experimentally observed low-temperature magnetic properties of the CMR manganates.<sup>9-11</sup> In broad terms, it is fair to say that *the CMR manganates are ferromagnetic<sup>19</sup> at  $x > 1/2$  and antiferromagnetic at  $x \leq 1/2$ .* Although the presence of narrow ferromagnetic regions (or possibly ferro-antiferromagnetic phase separation) at  $x < 1/2$  has been reported in some cases, the wide ferromagnetic area is always located at low hole doping,  $x > 1/2$ . The investigation of lightly-doped manganates with  $1-x \leq 0.1$  is complicated by the sample preparation issues. So far, only the 3D perovskite materials are available in this region; these are typically<sup>9,10</sup> found to remain ferromagnetic down to the very low values of  $1-x$ , with a likely exception of the  $x=1$  endpoint.<sup>20</sup> This is in contrast with robust Néel antiferromagnetic ordering, characteristic for all manganates at  $x \ll 1$ .

This qualitative discrepancy can be alleviated by taking into account the on-site Coulomb interaction,  $U$ . The latter does not affect the energy nor the carrier spectrum of the fully-magnetized half-metallic ferromagnetic state; however, when the neighboring spins (say,  $\vec{S}_i$  and  $\vec{S}_j$ ) are out of alignment, there arises a nonzero hopping matrix element,<sup>21</sup> connecting the conduction electron state at site  $i$  with the electron spin directed along  $\vec{S}_i$ , and the state at site  $j$  with the spin anti-aligned with  $\vec{S}_j$ . Thus, when two electrons are placed on sites  $i$  and  $j$ , there is a nonzero quantum-mechanical probability of double occupancy on-site, and the associated Coulomb energy: the electrons repel each other. Therefore, *Hubbard interaction enhances ferromagnetism*, and the strength of this effect increases with  $x$ .<sup>22</sup> Moreover, at a finite temperature  $T$ , when the ionic spins are misaligned due to thermal fluctuations, *an unusual  $T$ -dependent electron-electron repulsion arises in the ferromagnetic phase* (in Sec. III we will see that there also arises another, essentially many-body, contribution to the effective electron-electron interaction). We note that both of these effects, which we will consider in some detail below, are absent in the widespread simplified picture of double exchange, when the value of Hund's rule coupling is assumed to be infinite, making the double occupancy impossible.

Although  $U$  is, in fact, the largest energy scale in the problem, we will use the Hartree-Fock approximation, which formally becomes accurate only at small values of  $U/J_H$ . It is, however, expected that substituting larger values of  $U$  into our equations should yield the estimates which are adequate at the qualitative level. We note that in general, this "stretching" of the Hartree-Fock scheme requires some caution, as, for example, the energy of a single spin-down particle in the ferromagnetic state and in the presence of a partially filled spin-up band of width  $W \ll U$  is clearly of the order of  $J_H + W$ .<sup>23</sup> This is in contrast to the Hartree-Fock result for the energy of the spin-down electron,

$$\tilde{\epsilon}_k^{\downarrow} = \epsilon_k^{\uparrow} + J_S, \quad J_S = J_H + xU \quad (2)$$

[here,  $J_S$  is the mean-field (Stoner) band splitting]. However, the contribution of the Coulomb energy to the properties studied in the present paper originates from an integral over *many* inter-subband contributions (or over many spin-down electron states); it is hoped that the Hartree-Fock mean field-type approximation is more reliable in such a case.

We will be interested in the experimentally relevant case when the value of  $J_S$  is large in comparison to the Fermi energy,  $\epsilon_F$ . It should be noted that in this regime, the family of models with the Hamiltonian (1) and different values of the ratio  $xU/J_H$  provides a connection between the conventional double exchange system ( $U=0$ ) and the large- $U$  Hubbard model ( $J_H \rightarrow 0$ ). In fact, due to the considerable uncertainty in the values of  $t$  and  $J_H$  quoted in the literature, it is not clear whether  $J_H$  alone could always account for a complete carrier spin-polarization in the ferromagnetic state of the CMR manganates.<sup>14</sup> It is thus possible that in real systems, the half-metallic state (which at the mean-field level is implied by the condition  $J_S > \epsilon_F$ ) would not have been reached without further enhancement of band splitting by the

on-site Coulomb repulsion  $U$  [cf. Eq. (2)]. If this is indeed the case, it might lead to potentially important and novel many-body effects, at both zero and finite temperatures. These lie beyond the mean-field approach taken in the present work—within the Hartree-Fock scheme based on Eq. (2), it is indeed unimportant whether the perceived half-metallicity is partly due to the effects of Hubbard repulsion.

The spin wave theory of double exchange ferromagnets in the presence of on-site Coulomb repulsion is constructed in Sec. II. We evaluate the spin stiffness,  $D$ , and show that the on-site interaction *strengthens ferromagnetism*, while restoring the *correct asymmetry in the doping dependence* of  $D$ . In addition, we show that this interaction results in a *suppression of magnon energy near the zone boundary*, in comparison with the nearest-neighbor Heisenberg dispersion law. We then calculate the strength of the novel temperature-dependent electron-electron interaction (Sec. III). While this interaction appears negligible in the manganates, in case of lightly doped CMR magnetic semiconductors it does lead to an appreciable renormalization of nearest-neighbor Coulomb repulsion and (correlated) carrier hopping amplitude.

The effects of Hubbard repulsion on phase separation in double exchange magnets at  $T=0$  are discussed in Sec. IV. In the  $U=0$  case, the zero-temperature phase diagram (much like the doping dependence of spin-stiffness) suggests that the area of stability of the homogeneous ferromagnetic state is shifted towards the electron-doped end,  $x < 0.5$ , which is at variance with generic experimental observations (see above). We show that inclusion of  $U$  alleviates this difficulty as well.

The observed suppression of the carrier density of states near the Fermi level at low temperatures<sup>24</sup> is likely to be of the same origin as the much more pronounced depletion of the density of states<sup>25,26</sup> (sometimes termed “pseudogap”) in the vicinity of the Curie temperature. It appears, in turn, that in order to adequately describe the physics of CMR phenomenon one has to understand the nature of the pseudogap. It is therefore important that a proper description of a low-temperature ferromagnetic state of the CMR manganates should include the correct energy dependence of the density of states. In Sec. V we show that standard Altshuler-Aronov mechanism utilizing a combination of Coulomb repulsion (or the effective electron-electron interaction derived in Sec. III) and impurity scattering cannot account for the measured depletion of the density of states. This signals the insufficiency of our mean-field treatment in this case, and the presence of strong energy-dependent correlation effects even at low temperatures.

The implications of our findings are further summarized in Sec. VI, where we also discuss prospective directions for the future theoretical and experimental work in the field. On the whole, our results indicate that the effects of the Hubbard  $U$  are indeed crucial for the understanding of magnetic properties of the CMR compounds. Qualitatively, this suggests that in addition to the familiar double-exchange band-narrowing effects, the *correlated behavior of spin-polarized large- $U$  Hubbard carriers* should be recognized as an important mechanism underlying the physics of CMR compounds.

## II. SPIN WAVE THEORY

Low-temperature spin-wave properties of double exchange ferromagnets with  $U=0$  are well understood (see Ref.

27 and references therein). In parallel with Ref. 27, we begin our treatment of the Hamiltonian, Eq. (1) with  $U \neq 0$ , with the standard Holstein-Primakoff transformation, followed by a canonical transformation of the form

$$\mathcal{H} \rightarrow \mathcal{H}' = \exp(-W)\mathcal{H}\exp(W),$$

$$W = \frac{J_H}{\sqrt{2SN}} \sum_{\vec{k}, \vec{p}} (W_{\vec{k}, \vec{p}} c_{\vec{k}\uparrow}^\dagger c_{\vec{k}+\vec{p}\downarrow}^\dagger a_{\vec{p}}^\dagger - \text{H.c.}), \quad (3)$$

where  $a_{\vec{p}}^\dagger$  is the magnon creation operator, and  $N$  is the total number of lattice sites. The resulting Hamiltonian,  $\mathcal{H}'$ , takes form of a series in powers of  $1/\sqrt{S} \ll 1$ , with the leading-order term,

$$\mathcal{H}'_0 = \sum_{\vec{k}, \alpha} \epsilon_{\vec{k}}^\alpha c_{\vec{k}\alpha}^\dagger c_{\vec{k}\alpha} + U \sum_{\uparrow \neq \downarrow} c_{\uparrow}^\dagger c_{\downarrow}^\dagger c_{\uparrow} c_{\downarrow} + dNJ \quad (4)$$

(here,  $\Sigma'$  means that the quasimomentum conservation law is obeyed). Since we will be interested in the leading-order (classical) spin wave properties, we will need only the two further terms in this series. Here, in addition to the “usual” terms occurring already in the noninteracting model,<sup>27</sup>

$$\mathcal{H}'_1 = \frac{J_H}{\sqrt{2SN}} \sum_{\vec{k}, \vec{p}} \{ [W_{\vec{k}, \vec{p}} (\epsilon_{\vec{k}}^\uparrow - \epsilon_{\vec{k}+\vec{p}}^\downarrow) - 1] c_{\vec{k}\uparrow}^\dagger c_{\vec{k}+\vec{p}\downarrow}^\dagger a_{\vec{p}}^\dagger + \text{H.c.} \}, \quad (5)$$

$$\mathcal{H}'_2^{\text{eff}} = -\frac{J_H^2}{4SN} \sum_{\uparrow \neq \downarrow} \left\{ W_{1,3} W_{2,4} (\epsilon_{\uparrow}^\dagger - \epsilon_{\uparrow+3}^\dagger + \epsilon_{\downarrow}^\dagger - \epsilon_{\downarrow+4}^\dagger) - 2W_{1,3} - 2W_{2,4} - \frac{2}{J_H} \right\} c_{\uparrow}^\dagger c_{\downarrow}^\dagger a_{\uparrow}^\dagger a_{\downarrow}^\dagger - \frac{2J}{S} \sum_{\vec{k}} \left( d + \frac{1}{t} \epsilon_{\vec{k}} \right) a_{\vec{k}}^\dagger a_{\vec{k}} \quad (6)$$

(where  $W_{1,3}$  stands for  $W_{\vec{k}_1, \vec{k}_3}$ , etc., and the sum in the first term is over  $\vec{k}_1, \dots, \vec{k}_4$ ), we find two interaction-induced terms,

$$\mathcal{H}'_{i1}^{\text{eff}} = \frac{UJ_H}{\sqrt{2SN}^{3/2}} \sum_{\uparrow \neq \downarrow} \{ W_{1,5} c_{\uparrow}^\dagger c_{\downarrow}^\dagger c_{\uparrow} c_{\downarrow} a_{\uparrow}^\dagger + \text{H.c.} \}, \quad (7)$$

$$\mathcal{H}'_{i2}^{\text{eff}} = \frac{UJ_H^2}{4SN^2} \sum_{\uparrow \neq \downarrow} \{ W_{1,5} W_{4,6} - W_{2,5} W_{4,6} \} c_{\uparrow}^\dagger c_{\downarrow}^\dagger c_{\uparrow} c_{\downarrow} a_{\uparrow}^\dagger a_{\downarrow}^\dagger. \quad (8)$$

In writing Eqs. (6)–(8), we omitted the terms containing more than one spin-down fermion operator  $c_{\vec{k}\downarrow}$  or  $c_{\vec{k}\downarrow}^\dagger$  (hence the “eff” above the equality signs). Due to the absence of spin-down electrons in the half-metallic ferromagnetic ground state, these terms will not contribute to the quantities which are of interest to us here.

We find it advantageous to choose the coefficients  $W_{\vec{k}, \vec{p}}$  in such a way that the leading-order single-particle electron-magnon scattering,  $\mathcal{H}'_1$ , is cancelled by the average contribution of  $\mathcal{H}'_{i1}$  [see Fig. 1(a)]:

$$1 - (\epsilon_{\vec{k}}^\uparrow - \epsilon_{\vec{k}+\vec{p}}^\downarrow) W_{\vec{k}, \vec{p}} = -Ux W_{\vec{k}, \vec{p}} + \frac{U}{N} \sum_{\vec{q}} n_{\vec{q}} W_{\vec{q}, \vec{p}}, \quad (9)$$

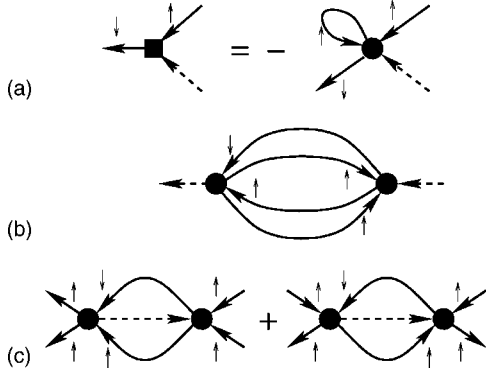


FIG. 1. (a) Schematic representation of Eq. (9), with the two vertices corresponding to  $\mathcal{H}'_1$  and  $\mathcal{H}'_{i1}$  [see Eqs. (5) and (7)], respectively. (b) Second-order interaction correction to the magnon energy [cf. Eq. (18)]. (c) Second-order contribution to the temperature-dependent interaction  $\Gamma^{\uparrow\uparrow}$  between two spin-up electrons; see Eq. (21). In all cases, solid and dashed lines correspond to electron and magnon Green's functions, respectively. Up- and down-arrows denote spin of the electrons. When evaluating these diagrams, one should ensure the proper antisymmetrization of the spin-up electronic "legs" of each vertex, taking into account the appropriate momentum dependence. Momentum integration is greatly simplified in the large- $J_S$  case considered here.

$$n_{\vec{k}} \equiv \langle c_{\vec{k}\uparrow}^\dagger c_{\vec{k}\uparrow} \rangle, \quad x = \frac{1}{N} \sum_{\vec{k}} n_{\vec{k}}. \quad (10)$$

Within the mean-field picture, condition (9) implies that the average number of magnons with a given momentum  $\vec{p}$ ,

$$\mathcal{N}_{\vec{p}} = \langle a_{\vec{p}}^\dagger a_{\vec{p}} \rangle, \quad (11)$$

remains constant.<sup>28</sup> In other words, it represents the optimal choice in separating the two distinct branches of excitations (magnons and electrons/holes).

Equation (9) is solved by

$$W_{\vec{k},\vec{p}} = \frac{R_{\vec{p}}}{\epsilon_{\vec{k}}^\uparrow - \epsilon_{\vec{k}+\vec{p}}^\downarrow - Ux}, \quad \frac{1}{R_{\vec{p}}} = 1 + \frac{U}{N} \sum_{\vec{q}} \frac{n_{\vec{q}}}{\epsilon_{\vec{q}}^\uparrow - \epsilon_{\vec{q}+\vec{p}}^\downarrow - Ux}, \quad (12)$$

which at  $U \rightarrow 0$  reduces to the familiar form,<sup>29</sup> used earlier for the noninteracting case.<sup>27,29</sup>

These expressions can be further simplified in the experimentally relevant case of  $J_S \gg \epsilon_F$ , where  $\epsilon_F = \mu + td$  is the Fermi energy, measured from the bottom of the spin-up subband. In particular, we then find

$$\frac{J_S}{R_{\vec{p}}} \approx J_H - \frac{U}{NJ_S} \sum_{\vec{q}} n_{\vec{q}} (\epsilon_{\vec{q}}^\uparrow - \epsilon_{\vec{q}+\vec{p}}^\downarrow) = J_H + \frac{|E|U}{J_S} \left( 1 + \frac{\epsilon_{\vec{p}}^\downarrow}{td} \right). \quad (13)$$

If we also restrict ourselves to the case of small magnon momenta,  $p, p' \ll 1$ , the second term on the rhs of Eq. (13) can be omitted, and we obtain

$$\mathcal{H}'_1 \approx \frac{Ux}{J_S \sqrt{2SN}} \sum_{\vec{k}, \vec{p}} \{ \vec{v}_{\vec{k}} \cdot \vec{p} c_{\vec{k}\uparrow}^\dagger c_{\vec{k}+\vec{p}\downarrow}^\dagger a_{\vec{p}}^\dagger + \text{H.c.} \}, \quad (14)$$

$$\mathcal{H}'_{i1} \approx \frac{U}{2\sqrt{2SN}^{3/2} J_S} \sum'_{1 \neq 4, \vec{p}} \{ (\vec{v}_1 - \vec{v}_2) \cdot \vec{p} c_{1\uparrow}^\dagger c_{2\uparrow}^\dagger c_{3\downarrow} c_{4\uparrow} a_{\vec{p}}^\dagger + \text{H.c.} \}, \quad (15)$$

$$\begin{aligned} \mathcal{H}'_{i2} \approx & \frac{U}{8SN^2 J_S^2} \sum'_{1 \neq 4, \vec{p}, \vec{p}'} \{ (\vec{v}_2 - \vec{v}_1) \cdot \vec{p} \} \{ (\vec{v}_3 - \vec{v}_4) \cdot \vec{p}' \} \\ & \times c_{1\uparrow}^\dagger c_{2\uparrow}^\dagger c_{3\uparrow} c_{4\uparrow} a_{\vec{p}}^\dagger a_{\vec{p}'}^\dagger, \end{aligned} \quad (16)$$

where  $\vec{v}_{\vec{k}} \equiv \partial \epsilon_{\vec{k}} / \partial \vec{k}$  is the electron velocity.

The spin-wave energy,  $\omega_{\vec{p}}$ , is equal to magnon self-energy,<sup>30</sup> which in turn can be evaluated perturbatively (in  $1/\sqrt{S}$ ). In addition to the first-order contributions from  $\mathcal{H}'_2$  and  $\mathcal{H}'_{i2}$ , there is a number of second-order corrections from  $\mathcal{H}'_1$  and  $\mathcal{H}'_{i1}$ . Owing to the condition (9), these second-order terms cancel each other, with the sole exception shown diagrammatically in Fig. 1(b). In drawing and evaluating this diagram, we make a drastic simplification of a mean-field type, corresponding to the Hartree decoupling of the interaction term in Eq. (4). Namely, we do not include any spin-up-spin-down electron vertices and use the expression

$$G_{\downarrow}(\omega, \vec{k}) = 1/(\omega - \epsilon_{\vec{k}} - J_S + \mu + i0 \cdot \text{sign } \omega), \quad (17)$$

for the spin-down electron Green's function. The Green's function for a spin-up electron in the half-metallic case is given by the usual formula,  $G_{\uparrow}(\omega, \vec{k}) = 1/(\omega - \epsilon_{\vec{k}} + \mu + i0 \cdot \text{sign } \omega)$ .

The resultant expression for long-wavelength magnon dispersion takes the usual form,  $\omega_{\vec{p}} = Dp^2$ , where the spin-stiffness  $D$  is given by

$$DS = \frac{|E|}{4d} - J - \frac{U^2 x(1-x) + J_S^2}{2dJ_S^3} \int n_{\vec{k}} v_{\vec{k}}^2 \frac{d^d k}{(2\pi)^d}. \quad (18)$$

The doping dependence of the spin-stiffness  $D$  for a two-dimensional system is illustrated in Fig. 2(a). Here, the solid line shows our result, Eq. (18), for  $J=0$  and experimentally relevant values  $J_H/t=5$ ,  $U/t=16$ . The effect of Hubbard repulsion becomes clear from a comparison with the dashed line, corresponding to the  $J_H/t=5$ ,  $U=0$  case.<sup>31</sup> We see that in the presence of the on-site repulsion, the magnitude of  $D(x)$  increases, and the maximum is shifted towards  $x > 0.5$ . The dashed-dotted line corresponds to the  $J_H/t=14.6$ ,  $U=0$  case, which is characterized by the same value of mean-field band-splitting  $J_S$  as  $J_H/t=5$ ,  $U/t=16$  system at the experimentally important value of electron density,  $x=0.6$ . While numerically the two results at  $0.5 < x < 0.8$  are relatively close, the dashed-dotted line possesses a larger slope, and still reaches a maximum below quarter-filling,  $x=0.5$ . For completeness, we note that the classical  $J_H \rightarrow \infty$  result (dotted line) is symmetric and corresponds to the largest magnitude of  $D(x)$ . We conclude that at a finite  $J_H$ , in addition to an overall increase in  $D$ , the inclusion of Hubbard repulsion leads to a relative increase of spin stiffness at  $x > 1/2$ , which

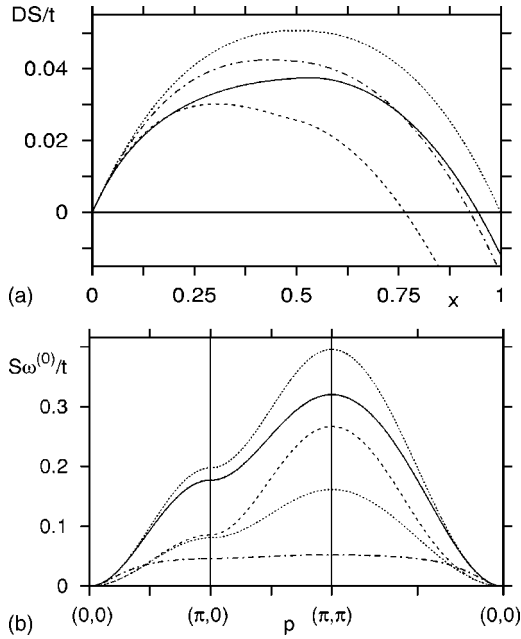


FIG. 2. (a) Doping dependence of spin stiffness for a two-dimensional system with  $J=0$ ,  $J_H/t=5$  (solid and dashed lines, corresponding to  $U/t=16$  and  $U=0$  cases, respectively). The dashed-dotted line corresponds to  $J_H/t=14.6$  and  $U=0$ , and the dotted line—to  $J_H \rightarrow \infty$ . (b) The leading-order magnon energy in a 2D system with  $U/t=16$ ,  $J=0$ , and  $x=0.6$ . The solid, dashed and the upper dotted lines are plotted using Eq. (19) and correspond to  $J_H/t=5$ ,  $J_H/t=0.2$  and  $J_H \rightarrow \infty$ , respectively. The dashed line is the result<sup>43</sup> for  $J_H/t=5$ ,  $U=0$ , and the lower dotted line is the corresponding Heisenberg fit.

is consistent with the experimental observation that the ferromagnetic tendencies in the CMR manganates are more pronounced in this doping region. We note that an earlier mean field study<sup>7</sup> of the effects of the Hubbard repulsion on the Curie temperature,  $T_C(x)$ , suggested somewhat similar trends.

The overall increase of spin stiffness originates from the mean-field effects discussed in Sec. I and corresponds to substitution  $J_H \rightarrow J_S$  in the last term of Eq. (18). Since  $J_S > J_H$ , the (negative) pre-factor in front of the (positive) integral decreases in comparison with the  $U=0$  case, resulting in the increase of  $D$ . At sufficiently low values of  $x$ , however, this tendency is counter-balanced by effects of the Hubbard correlations, which contribute the quantity  $U^2x(1-x)$  to the numerator of this pre-factor. The underlying physics will be discussed in Sec. III; here we merely note that as a result, the spin stiffness well below the quarter-filling,  $x < 0.2$ , may actually be somewhat suppressed in comparison with the  $U=0$  value. For the case of  $J_H=5t$ ,  $U=16t$ , this takes place for  $x < 0.19$  [see Fig. 2(a)].

As for a quantitative comparison of our results for  $D(x)$  at  $x > 0.5$  with the experimental data for the CMR manganates, this appears problematic due to a number of reasons: (i) available experimental results on the doping dependence of spin-stiffness<sup>32</sup> are still incomplete; (ii) it is known<sup>27</sup> that quantum corrections, not included in Eq. (18), lead to an appreciable renormalization of spin stiffness magnitude; and

(iii) the values of band (and orbital) structure parameters and direct exchange integrals for particular compounds are known with a large degree of uncertainty. Nevertheless, it is adequate to say that qualitatively, both the overall profile and the magnitude of spin-stiffness, as given by Eq. (18), are consistent with the experimental results for  $D(x)$  within the metallic ferromagnetic region,  $0.2 < 1-x < 0.5$ .

When spin stiffness [as shown in Fig. 2(a) for  $J=0$ ] turns negative, the ferromagnetic ground state can only be stabilized by including a sufficiently strong direct ferromagnetic exchange coupling,  $J < 0$ . On the contrary, a positive value of spin stiffness does *not* guarantee the stability of a uniform ferromagnetic ground state, since the latter might still be unstable with respect to phase separation (see Sec. IV).

Within the mean-field approach taken here, expression (18) is expected to hold at  $J_S \gg \epsilon_F$  for all values of the ratio  $U/J_H$ , except for the  $J_H \rightarrow 0$  case of a pure Hubbard model. In this case, the ionic spins are fully decoupled from the itinerant ones, and the leading-order (in  $1/S$ ) term in the magnon energy vanishes. Formally, at  $J_H \rightarrow 0$  the second term on the rhs of Eq. (13) cannot be omitted even for small  $p$ , and Eqs. (14)–(18) become invalid. We note that if the value of  $U$  is sufficiently large, the conduction electrons may still be in the fully spin-polarized ferromagnetic state as expected for a partially-filled Hubbard model below half-filling,  $x < 1$ . While this is always the case within the present mean-field treatment, the actual identification of the stability region for a ferromagnetic state of a large- $U$  Hubbard model remains an open problem.<sup>33,34</sup> Although this subject is well beyond the scope of the present work, it is important to note that (i) it is likely that over a broad range of doping values, the instability of the fully spin-polarized state of the Hubbard model ( $J_H=0$ ) results only in a *partial* reduction of magnetization,<sup>33</sup> and (ii) it is possible that allowing for a small but finite value of  $J_H$  greatly enhances stability of the fully spin-polarized state (cf. Ref. 34).

In view of relatively small values of  $J_H$ , reported in the bandstructure calculations, it is important to study the crossover to the free-spin ( $J_H \rightarrow 0$ ) case in some detail. The leading-order (in both  $\epsilon_F/J_S$  and  $1/S$ ) term in the magnon energy originates from  $\mathcal{H}'_2$  and in the absence of a direct coupling  $J$  has the form

$$\omega_{\vec{p}}^{(0)} = \frac{|E|}{2S} \left( 1 + \frac{\epsilon_{\vec{p}}}{td} \right) \frac{J_H^2 + xJ_H \frac{|E|U^2}{J_S^2} \left( 1 + \frac{\epsilon_{\vec{p}}}{td} \right)}{\left[ J_H + \frac{|E|U}{J_S} \left( 1 + \frac{\epsilon_{\vec{p}}}{td} \right) \right]^2}. \quad (19)$$

Here, momentum  $\vec{p}$  is allowed to take any value within the Brillouin zone. When  $J_H$  is sufficiently small, the second term in the denominator dominates,<sup>35</sup> provided that  $p^2 \gtrsim (J_S J_H)/(U|E|)$ . The magnon energy then saturates at a constant value,  $\omega_{\vec{p}} = xJ_H/(2S)$ , which is consistent with a physical picture of independent ionic spins  $\vec{S}_i$  subject to an effective magnetic field of the magnitude  $xJ_H/2$ . The latter is created by the rigid ferromagnetic Fermi sea of the large- $U$  Hubbard carriers.<sup>36</sup> This situation is illustrated by a dashed-dotted line in Fig. 2(b), corresponding to  $J_H/t=0.2$ ,  $U/t$

$=16$  and  $x=0.6$ . While for the experimentally relevant value of  $J_H/t=5$  (solid line) spin-wave energy does not reach saturation, the effects of suppression of the magnon energy (in comparison with the pure cosine Heisenberg law—see the upper dotted line, corresponding to  $J_H \rightarrow \infty$ ) are still felt near the zone boundary.<sup>37</sup> These become more pronounced (possibly leading even to a local minimum of spin-wave dispersion at the point  $\vec{p}=\{\pi, \pi\}$ ), if a direct antiferromagnetic coupling  $J>0$  between the ionic spins is taken into account. The latter gives rise to an extra term,  $-2J(\epsilon_{\vec{p}}+td)/(tS)$ , which should be added to the rhs of Eq. (19). Thus, *at the moderate values of  $J_H$  within the experimentally relevant range, the spin-wave dispersion in a double exchange ferromagnet with a large on-site repulsion  $U$  shows zone-boundary “softening” in comparison with the nearest-neighbor Heisenberg dispersion law.* There has been an extensive theoretical effort<sup>38,39</sup> directed at understanding this property, which is observed experimentally<sup>40</sup> in many (but not all<sup>41</sup>) CMR compounds. It is important that this generic feature is recovered within the present model, as suggested by earlier variational studies<sup>39</sup> of the effects of  $U$  on the magnon dispersion.

We note that this zone-boundary softening effect occurs in both two and three dimensions, and is entirely due to the Hubbard repulsion,  $U$ . Indeed, for any dimensionality  $d$  it can be shown<sup>42</sup> that at  $U=0$  and  $x>0.5$ , the magnon dispersion at sufficiently large  $J_H \gtrsim \epsilon_F$  *hardens* towards the zone boundary. This is illustrated by the dashed line in Fig. 2(b), representing the  $J_H=5t$ ,  $U=0$  case.<sup>43</sup> One can see that at large momenta, the corresponding Heisenberg dispersion law,  $\omega_{\vec{p}}=2D(td+\epsilon_{\vec{p}})/t$  with the appropriate value of spin-stiffness  $D$ , indeed yields lower magnon energies (lower dotted line).

### III. EFFECTIVE ELECTRON-ELECTRON INTERACTION

The original on-site Coulomb repulsion, as represented by the last term in Eq. (1), acts between electrons with anti-aligned spins. As the average number of spin-down electrons in a half-metallic double exchange ferromagnet at low temperatures is negligible, it might seem that the spin-up electrons remain noninteracting even in the presence of the Hubbard  $U$ . However, as already discussed in Sec. I, at finite temperatures the on-site repulsion also gives rise to an interaction between electrons with the same sign of spin projection. The presence of this novel interaction,  $V_{eff}$ , is clear, e.g., from the form of the operator  $\mathcal{H}'_{i2}$  [see Eq. (8)], which at finite  $T$  can be averaged over the equilibrium magnon distribution. Another contribution<sup>44</sup> to  $V_{eff}$  originates from the second-order processes, involving various combinations of terms from  $H'_1$  and  $H'_{i1}$ , Eqs. (5) and (7). As in Sec. II, the condition (9) leads to a massive cancellation among these second-order diagrams [cf. Fig. 1(a)], with the only two surviving terms shown in Fig. 1(c).

In Fig. 1(c), vertices correspond to the magnon-electron interaction,  $\mathcal{H}'_{i1}$ , and the solid lines are finite-temperature electron Green's functions,

$$\mathcal{G}_\uparrow^{-1}(\zeta, \vec{p}) = i\zeta - \epsilon_{\vec{p}} + \mu, \quad \mathcal{G}_\downarrow^{-1}(\zeta, \vec{p}) = i\zeta - \epsilon_{\vec{p}} - J_S + \mu, \quad (20)$$

where we again used the Hartree mean-field form for  $\mathcal{G}_\downarrow$  [cf. Eq. (17)]. At low temperatures,  $T \ll D$ , only the long-

wavelength magnons are present, and the magnon Green's function can be written as  $\mathcal{G}_m^{-1} \approx i\zeta - Dp^2$ . Here, the spin stiffness  $D$  can be evaluated with the help of Eq. (18) or taken directly from the low-temperature neutron scattering measurements. Furthermore, at low temperatures Eqs. (15) and (16) may be used in place of Eqs. (7) and (8).

To leading order in  $\epsilon_F/J_S$  and  $1/S$ , the net result for the vertex function,  $\Gamma_{12,43}^{\uparrow\uparrow}$ , of two spin-up electrons scattering is given by the expression

$$\begin{aligned} & \frac{2}{SJ_S^2} \int \frac{d^d p}{(2\pi)^d} \mathcal{N}_{\vec{p}} \left[ U(\vec{v}_1 \cdot \vec{p})(\vec{v}_4 \cdot \vec{p}) - \frac{U^2(x-1)}{i(\zeta_1 + \zeta_2) - J_S} \right. \\ & \quad \times (\vec{v}_1 \cdot \vec{p})(\vec{v}_4 \cdot \vec{p}) - \frac{U^2}{i(\zeta_1 - \zeta_3) - J_S} \\ & \quad \left. \times \int \frac{n_{\vec{k}} d^d k}{(2\pi)^d} \{(\vec{v}_1 - \vec{v}_{\vec{k}}) \cdot \vec{p}\} \{(\vec{v}_4 - \vec{v}_{\vec{k}}) \cdot \vec{p}\} \right], \quad (21) \end{aligned}$$

which should be anti-symmetrized<sup>45</sup> with respect to the velocities and frequencies of the outgoing (incoming) electrons,  $\vec{v}_{1,2} \equiv \partial \epsilon_{\vec{p}_{1,2}} / \partial \vec{p}_{1,2}$  and  $\zeta_{1,2}$  ( $\vec{v}_{3,4}$  and  $\zeta_{3,4}$ ). In Eq. (21), the first term in brackets represents the first-order contribution of the operator  $\mathcal{H}'_{i2}$ , Eq. (16), whereas the other two terms come from the two diagrams shown in Fig. 1(c);  $\mathcal{N}_{\vec{p}} = [\exp(Dp^2/T) - 1]^{-1}$  is the average magnon occupation number, Eq. (11).

The retardation (frequency-dependence) effects in  $\Gamma^{\uparrow\uparrow}$  become noticeable only on a very large electron energy (frequency) scale<sup>46</sup> of  $|\zeta_i| \sim J_S$ , and can be omitted whenever only electrons with energies near the Fermi level are considered. In this case, the effect of electron-electron scattering as described by the vertex  $\Gamma^{\uparrow\uparrow}$  is equivalent to that of an *effective electron-electron interaction* of the form

$$\begin{aligned} V_{eff} = & - \frac{U[J_S + U(2x-1)]}{8dSJ_S^3 N} \int p^2 \mathcal{N}_{\vec{p}} \frac{d^d p}{(2\pi)^d} \\ & \times \sum'_{1+4} (\vec{v}_1 - \vec{v}_2) \cdot (\vec{v}_3 - \vec{v}_4) c_{1\uparrow}^\dagger c_{2\uparrow}^\dagger c_{3\uparrow} c_{4\uparrow}, \quad (22) \end{aligned}$$

where we also used the fact that the long-wavelength magnon dispersion is isotropic. In the case of small  $U \ll J_H$ ,  $\epsilon_F$ , our mean-field results, Eqs. (21) and (22), can be re-derived within the perturbation theory in  $U$ . As expected on physical grounds,  $V_{eff}$  vanishes also in the  $U \rightarrow \infty$  limit, when the double occupancy on-site is forbidden. The momentum integral occurring on the rhs of Eq. (22) can be easily evaluated,

$$\begin{aligned} I(T) \equiv & \int p^2 \mathcal{N}_{\vec{p}} \frac{d^d p}{(2\pi)^d} \\ = & \begin{cases} \frac{3\zeta(5/2)}{16\pi^{3/2}} \left(\frac{T}{D}\right)^{5/2} & \text{in three dimensions,} \\ \frac{\pi}{24} \left(\frac{T}{D}\right)^2 & \text{in two dimensions,} \end{cases} \quad (23) \end{aligned}$$

where  $\zeta(5/2) \approx 1.34$  is the Riemann's *zeta*-function. We note that the quantity (23) can also be expressed macroscopically as the thermal average of

$$\frac{1}{2S} \sum_{\alpha=1}^3 \{ \vec{\nabla} M^\alpha \cdot \vec{\nabla} M^\alpha \}, \quad (24)$$

where  $M^\alpha$  are the three components of local magnetization,<sup>47</sup>  $\vec{M}$ . This shows that the appearance of  $V_{eff}$  is indeed a direct consequence of the misalignment of neighboring spins (which in turn is due to the thermal fluctuations; cf. Sec. I).

Although the precise form of  $V_{eff}$  in Eq. (22) obviously has only a mean-field validity, we emphasize that qualitatively this effect, which has a clear physical origin, will survive in an exact treatment. If anything, the mean-field approach yields a smaller magnitude of  $V_{eff}$ : indeed, Eqs. (20) overestimate the energy of a spin-down electron, which enters into the denominators of diagrammatic expressions in Fig. 1(c).

Thus, we conclude that *with increasing temperature  $T$ , there arises an effective interaction between the spin-polarized carriers in a double exchange ferromagnet with  $U > 0$* . For the purposes of order-of-magnitude estimates, one can assume that electron dispersion is isotropic,  $\vec{v} \approx \vec{p}/m_*$ , where  $m_*$  is an effective mass of electron (or hole). The interaction, Eq. (22), then takes form of a simple  $p$ -wave scattering,

$$V_{eff} = \frac{2}{Nm_*^2} \sum_{\vec{s}, \vec{q}, \vec{q}'} V(T) (\vec{q} \cdot \vec{q}') c_{\vec{s}+\vec{q}'\uparrow}^\dagger c_{\vec{s}-\vec{q}'\uparrow}^\dagger c_{\vec{s}-\vec{q}\downarrow} c_{\vec{s}+\vec{q}\downarrow}, \quad (25)$$

with

$$V(T) = \frac{U[J_S + U(2x-1)]}{4dSJ_S^3} I(T). \quad (26)$$

In real space, the effective interaction, Eq. (22), takes form

$$V_{eff} = \frac{1}{2} t^2 V(T) \sum_{i,\Delta} \{ c_{i\uparrow}^\dagger c_{i+\Delta\uparrow}^\dagger c_{i+\Delta\uparrow} c_{i\uparrow} - c_{i+\Delta\uparrow}^\dagger c_{i\uparrow}^\dagger c_{i\uparrow} c_{i-\Delta\uparrow} \}. \quad (27)$$

Here, for each lattice site  $i$  a summation over its  $2d$  nearest neighbors (labeled  $i+\Delta$ ) is performed. The first term in Eq. (27) contains a product of carrier densities; it renormalizes the “bare” repulsion between electrons on the neighboring sites, which is present in reality but not included in our model, Eq. (1). In the case of the CMR manganates, this bare repulsion is expected<sup>48</sup> to be of the order of  $V_{nn} \geq 0.05$  eV; on the other hand, the value of  $V(T)$  as found from Eq. (26) with  $U=8$  eV,  $t=0.5$  eV,  $J_H=2.5$  eV and  $x=0.6$  is  $t^2 V(T) \sim 10^{-4} (T/T_C)^{5/2}$  (in units of eV, for the 3D case; we also assumed that the Curie temperature  $T_C$  is of the order of the zero-temperature spin-stiffness,  $D$ ). We thus see that in the manganates, the contribution of  $V_{eff}$ , Eq. (27), to the nearest-neighbor repulsion remains negligible even for  $T \sim T_C$ .

The situation is likely to be very different for nonmanganate magnetic semiconductors exhibiting CMR. It is expected<sup>49,50</sup> that in the lightly doped ( $x \sim 10^{-4}$ ) EuSe, EuTe, EuO or undoped (semimetallic) EuB<sub>6</sub> the parameters of the Hamiltonian, Eq. (1) can be roughly estimated as  $U=7$  eV,  $J_H=0.4$  eV and  $t=0.5$  eV. Taking also into account the mag-

nitude of Eu spin ( $7/2$ ), we find  $t^2 V(T) \sim -0.2 (T/T_C)^{5/2}$  in units of eV. Thus, the effects of temperature-dependent renormalization of  $V_{nn}$  in these compounds may be appreciable.

We note that in the latter example, the sign of  $V(T)$  is negative, corresponding to an effective *attraction* between electrons on the neighboring sites. This clearly contradicts the simple physical picture outlined in Sec. I (based on the small- $U$  perturbative considerations). Indeed, as can be seen from Eq. (26), at sufficiently large values of  $U$  the effective interaction can in fact become attractive. This occurs when the second term in the numerator,  $U(2x-1)$ , which is negative for  $x < 0.5$ , dominates over the first one. We suggest that this second term, which originates from the two diagrams shown in Fig. 1(c), is due to the many-body effects.

Indeed, the large- $U$  partially-filled Hubbard conduction band has (at least within the mean-field picture—see the discussion in Sec. II) the ferromagnetic tendencies of its own, which are unrelated to the ionic spins and double exchange. In the  $J_H=0$  case, the ferromagnetic, fully spin-polarized state of the carriers (uncoupled to the ionic spins) corresponds to the largest bandwidth and hence to the lowest kinetic energy. Let us now assume that the value of  $J_H$  is finite and the ionic spins are fixed in a certain configuration which is not perfectly ferromagnetic (in the present context, the deviation of the ionic spin configuration from the ferromagnetic ground state is due to the thermal fluctuations). The electron bandstructure is then determined by a competition between the Hubbard band ferromagnetism (which favors a uniform ferromagnetic alignment of the carrier spins and hence decoupling from the ionic spin background) and the Hund’s rule coupling (which tends to align the carrier spins locally with the ionic ones, leading to the double exchange band narrowing).<sup>51</sup> Not surprisingly for an interacting many-body system, the resulting bandstructure (along with the local carrier spin direction and the overall strength of band ferromagnetism) therefore depends on the bandfilling  $x$ . As a result of electron-electron interaction, the mean-field bandwidth of spin-polarized carriers (somewhat suppressed due to the double exchange mechanism) then increases whenever the bandfilling of electrons (or holes) is increased, reaching the maximum at  $x=0.5$  (where the effects of Hubbard band ferromagnetism are most pronounced). The kinetic energy of an electron at a sufficiently small value of  $x$  may thus be lowered if another electron is present nearby (a local increase of the carrier density), leading to the effective attraction.

This effect is likely to have important physical consequences in the case of Eu-based magnetic semiconductors, as the effective attraction will further improve the stability of microscopic droplet-like areas with increased carrier density and enhanced ferromagnetic order (ferrons<sup>2</sup>), which were argued<sup>2,52</sup> to play a key role in these compounds. If the bare nearest-neighbor Coulomb repulsion is not too strong (which is expected), taking the effective interaction into account may in fact lead to the total nearest neighbor interaction being attractive above a certain temperature. This in turn might signal an instability of the homogeneous ferromagnetic state and possibly the formation of ferrons. This question obviously calls for further investigation.

The second term in Eq. (27) is a variant of *correlated*

*electron hopping.* While the effects of this term in the present context are not immediately clear, we note that correlated hopping represents a much-studied extension of the Hubbard model. In fact, an effective interaction somewhat similar to (27) (although involving fermions with antiparallel spins) has been obtained in the past<sup>53</sup> within a mean-field approach to a large- $U$  Hubbard model. In the case of CMR manganates, where the quantity  $V(T)$  is very small, the effects of the correlated hopping term in Eq. (27) are expected to be negligible. Again, the situation can be very different for the CMR magnetic semiconductors with small carrier densities.

We note that while the result (27) applies only for degenerate magnetic semiconductors with finite carrier densities at  $T \rightarrow 0$ , we expect a similar magnon-mediated effective electron-electron interaction to arise in the nondegenerate (undoped) case as well.

#### IV. PHASE SEPARATION AND PHASE DIAGRAM AT $T=0$

Although spin stiffness  $D(x)$  and spin-wave energy,  $\omega_p$ , discussed in Sec. II, are important and much-studied quantities characterizing magnetic properties of double exchange ferromagnets, their behavior is not expected to yield any conclusive information on the stability of the ferromagnetic state at low temperatures. Indeed, for large  $J_H$  and  $U=0$  it is possible to verify (see, e.g., Ref. 18 and references therein) that, in a marked difference from conventional isotropic insulating magnets with competing interactions, the zero-temperature magnon spectrum of a double exchange magnet in the homogeneous ferromagnetic state does not soften when the latter is rendered unstable due to a change in the balance between ferro- and antiferromagnetic tendencies in the system. This is because phase separation, which is a generic phenomenon found in both experimental and theoretical studies of the CMR manganates and doped magnetic semiconductors<sup>2,17</sup> always preempts a second-order, spin wave-mediated phase transition. On the theory side, there is little doubt that this situation persists in the finite- $J_H$ ,  $U > 0$  case in two and three dimensions (in particular, this is known to be true in the  $J_H \rightarrow 0$ , large- $U$  case of the pure Hubbard model<sup>54</sup>). In the present section, we will see how the presence of on-site Coulomb repulsion  $U$  affects the physics of phase separation and, in particular, the low-temperature phase diagram. We note that the effects of Coulomb repulsion on phase separation in this model were studied in Ref. 4 within a somewhat different mean-field approach.

At a given value of electron band filling  $x$  [and the corresponding chemical potential,  $\mu(x)$ ], the homogeneous ferromagnetic phase of a double exchange magnet is unstable with respect to phase separation whenever its thermodynamic potential,

$$\Omega_{FM}[\mu(x), J] = E - \mu x + dJ, \quad E = \int \epsilon_{\vec{k}} n_{\vec{k}} \frac{d^d k}{(2\pi)^d}, \quad (28)$$

is larger than the thermodynamic potential  $\Omega_P$  of another homogeneous phase  $P$ , calculated at the same value of  $\mu$ . The total energy of the system can then be lowered if areas of this new phase are formed within the bulk of the

ferromagnet.<sup>55</sup> Therefore in order to find the stability region of the homogeneous ferromagnetic phase, one has to identify the relevant phases and evaluate the dependence of their respective thermodynamic potentials on the parameters of the Hamiltonian, Eq. (1).

For any given values of  $J_H$  and  $U$ , it is convenient to characterize the stability of the homogeneous ferromagnetic state by the critical value of direct antiferromagnetic exchange coupling,  $J_{cr}(x)$ , above which the system becomes phase-separated. The calculation thus proceeds as follows: the equation,

$$\Omega_{FM}[\mu(x), J_P] = \Omega_P[\mu(x), J_P], \quad (29)$$

is solved for several possible phases  $P$ , yielding the corresponding values of  $J = J_P(x, U, J_H)$ . At a fixed  $x$ , the value of  $J_{cr}$  is then given by the lowest  $J_P$ . Such a procedure clearly has a variational validity as it does not imply an existence of a rigorous proof that  $J_{cr}$  cannot be lowered further by broadening our selection of phases  $P$ . On the other hand, the condition  $J > J_{cr}$  is obviously *sufficient* for the phase separation to occur. We shall now turn to the two possible antiferromagnetic phases considered in the present paper.

Based on the numerous results for the  $U=0$  case,<sup>2,18,17</sup> one expects that a phase separation into ferromagnetic and the usual *Néel antiferromagnetic* (*G-type antiferromagnetic*) phase, corresponding to the wave vector of  $\{\pi, \pi, \pi\}$  (in two dimensions,  $\{\pi, \pi\}$ ) takes place in the vicinity of endpoints,  $x=0$  and  $x=1$ . To leading order in  $1/S$ , one can use the classical formalism [see, e.g., Eqs. (9) and (10) of Ref. 15] to re-write the Hamiltonian in terms of the new fermions  $d_{i\uparrow}$  (and  $d_{i\downarrow}$ ), whose spins are aligned (antialigned) with the local ionic spins  $\vec{S}_i$  in the *G*-type antiferromagnet:

$$\begin{aligned} \mathcal{H}_G = & -\frac{t}{2} \sum_{\langle i,j \rangle} (d_{i\downarrow}^\dagger d_{j\uparrow} + d_{i\uparrow}^\dagger d_{j\downarrow} + \text{H.c.}) + \frac{J_H}{2} \sum_i (d_{i\downarrow}^\dagger d_{i\downarrow} - d_{i\uparrow}^\dagger d_{i\uparrow}) \\ & - dJN + U \sum_i (d_{i\uparrow}^\dagger d_{i\uparrow} x_{\downarrow} + d_{i\downarrow}^\dagger d_{i\downarrow} x_{\uparrow} - x_{\uparrow} x_{\downarrow}). \end{aligned} \quad (30)$$

Here, a standard Hartree mean-field decoupling has been carried out in the last term, with  $x_{\alpha} \equiv \langle d_{i\alpha}^\dagger d_{i\alpha} \rangle$  denoting the average spin-up and spin-down fermion densities. Upon Fourier transformation and diagonalization (see the Appendix), Eq. (30) takes the form

$$\mathcal{H} = \sum_{\vec{k}, \alpha} \epsilon_G^\alpha(\vec{k}) f_{\vec{k}, \alpha}^\dagger f_{\vec{k}, \alpha} - dNJ - UNx_{\downarrow}x_{\uparrow}. \quad (31)$$

Here,  $f_{\vec{k}, \alpha}^\dagger$  are the new fermion creation operators, the momentum summation is performed over the full (ferromagnetic) Brillouin zone, and the carrier spectrum is given by

$$\epsilon_G^{\uparrow, \downarrow}(\vec{k}) = \delta \mp \sqrt{\frac{1}{4}(J_S^{(G)})^2 + (\epsilon_{\vec{k}})^2}, \quad (32)$$

$$J_S^{(G)} = J_H + U(x_{\uparrow} - x_{\downarrow}), \quad \delta = \frac{1}{2}U(x_{\uparrow} + x_{\downarrow}). \quad (33)$$

These equations are valid also at  $U=0$ , in which case  $J_S^{(G)} = J_H$  and  $\delta=0$ . For general values of  $U$ , the quantity  $J_S^{(G)}$  represents the Stoner-type mean-field band splitting in the



$G$ -antiferromagnetic phase, whereas  $\delta$  merely renormalizes the chemical potential,  $\mu - \frac{1}{2}J_H$ . The closed system of mean field equations for these parameters of the  $G$ -antiferromagnetic phase at a given band filling,  $x_G = x_\uparrow + x_\downarrow$ , is presented and discussed in the Appendix. As we are interested only in finding the phase-separation instability of the homogeneous ferromagnetic state, we do not need to solve these mean-field equations for general values of  $x_G$ . The latter will rather be determined by  $\mu$ , which in turn is related in a usual way to the band filling  $x$  of the homogeneous double exchange ferromagnet.

When the value of  $x$  is small, the chemical potential in the ferromagnetic phase lies below the bottom of the lower band of  $G$ -antiferromagnet [given by Eq. (32) with  $x_\uparrow = x_\downarrow = 0$ ],

$$\mu(x) < \mu_0 = \frac{1}{2}J_H - \sqrt{\frac{1}{4}J_H^2 + t^2d^2}, \quad (34)$$

and the thermodynamic potential of the Néel phase,  $\Omega_G$ , equals  $-dJ$ . As the value of  $x$  increases, the inequality (34) is eventually violated, giving rise to a nonzero carrier density  $x_G$  (with  $x_\uparrow > x_\downarrow$ ) in the antiferromagnetic phase.

For the realistic values of parameters in the 2D case, we find that the  $G$ -antiferromagnetic phase with partially-filled band,  $0 > x_G > 1$ , is not relevant in the context of phase separation. This is because within the corresponding range of values of  $x$  [and  $\mu(x)$ ], the critical value of superexchange coupling,  $J_G(x)$ , is larger than the one which corresponds to the second-order spin-wave transition,  $J_{sw}(x) = D_0(x)S$  (where  $D_0$  is the spin stiffness evaluated at  $J=0$ ). The peculiar properties of the partially-filled case, as discussed in the Appendix, are interesting on their own, and may also prove relevant in another context. Here, we will turn to the case when the chemical potential  $\mu(x)$  lies above the top of the filled  $G$ -antiferromagnetic band,

$$\mu(x) > \frac{t^2dU}{2(J_H + U)^2}, \quad (35)$$

resulting in  $x_G = 1$ . Given the realistic (large) magnitude of  $U$ , the value of  $J_S^{(G)} \approx J_H + U$  is then also large, and the mean-field equations are readily solved with the help of the  $t/J_S^{(G)}$ -expansion [which was used also in writing Eq. (35)]. We find an expression

$$\Omega_G = -\frac{t^2d}{2(J_H + U)} - \mu(x) - dJ, \quad (36)$$

which can be used to determine the critical value of superexchange  $J_G(x)$  whenever the phase separation into the partially filled ferromagnetic and filled ( $x_G = 1$ ) Néel states becomes possible. As we will see below, this happens only well above the quarter-filling of the ferromagnetic band,  $x > 0.5$ , where the inequality (35) is clearly satisfied.

Another phase which seems to be ubiquitous in the 2D case is the  $A$ -type antiferromagnetic one, characterized by the wave vector  $\{\pi, 0\}$ . The mean-field theory of the  $A$ -antiferromagnetic phase is formulated along the same lines as for the Néel antiferromagnet above, where Eq. (32) is now replaced with

$$\epsilon_A^{\uparrow, \downarrow}(\vec{k}) = \delta - t \cos k_x \mp \sqrt{\frac{1}{4}(J_S^{(A)})^2 + t^2 \cos^2 k_y}, \quad (37)$$

and the (negative) superexchange term in the Hamiltonian is cancelled. In spite of the higher superexchange energy, the  $A$ -type phase becomes more profitable than the Néel one because it allows for a larger gain in the kinetic energy of carriers. Thus, it is clear that the  $A$ -phase becomes relevant only when the carrier density in the  $A$ -type ferromagnet  $x_A[\mu(x)]$  (and similarly, the hole density,  $1 - x_A$ ) is not too small. In case of large  $U$ , this means that the value of Stoner bandsplitting,  $J_S^{(A)}$ , is much larger than the hopping matrix element,  $t$ .

Therefore while for moderate values of  $U$  the full system of mean field equations for  $J_S^{(A)}$  and  $x_A$  must be solved, and then the thermodynamic potential,

$$\Omega_A = \int \left\{ \epsilon_A^{\uparrow}(\vec{k}) + \frac{1}{2}J_H - \mu(x) \right\} n_k^{(A)} \frac{d^2k}{4\pi^2} - \frac{1}{4}Ux_A^2 + \frac{1}{4U}(J_S^{(A)} - J_H)^2 \quad (38)$$

[where  $n_k^{(A)}$  is the Fermi distribution function, corresponding to the dispersion law (37) and chemical potential  $\mu(x) - J_H/2$ ], must be evaluated numerically, in the large- $U$  case it is sufficient to retain the leading-order terms in  $t/J_S^{(A)}$ . In this way we obtain for  $U \gg t$ ,

$$J_S^{(A)} \approx J_H + Ux_A \approx J_H + \frac{U}{\pi} \left[ \pi - \arccos \frac{\mu(x)}{t} \right], \quad (39)$$

$$\Omega_A \approx -\frac{1}{\pi} \sqrt{t^2 - \mu^2} - \frac{1}{\pi} \left( \mu + \frac{t^2}{2J_S^{(A)}} \right) \left( \pi - \arccos \frac{\mu}{t} \right). \quad (40)$$

Equations (39) and (40) hold for  $|\mu(x)| < t$ , which at large  $U$  corresponds to partial filling of the  $A$ -antiferromagnetic band.

The zero-temperature phase diagram for a 2D system with  $J_H/t = 5$  and  $U = 0$  is shown in Fig. 3(a). Here, the (upper) dotted line corresponds to the long-wavelength spin-wave softening,  $J_{sw}(x) = D_0(x)S$ ; at  $x < 0.31$ , it is preempted by spin wave instability at  $\vec{p} = \{\pi, \pi\}$  (lower dotted line). Phase separation instabilities involving Néel and  $A$ -type antiferromagnetic phases are represented by solid and dashed lines, respectively. We see that the stability region of the uniform ferromagnetic phase is heavily shifted towards the electron-doped end,  $x < 0.5$ ; at the experimentally relevant values of  $J/t \sim 0.015$  ( $J/t \sim 0.02$ ), the homogeneous ferromagnetic state is unstable everywhere at  $1 - x < 0.34$  ( $1 - x < 0.55$ ). As explained in the Introduction, it is at  $x > 0.5$  that the broad low-temperature ferromagnetic region is found for the CMR manganates, and such an instability clearly contradicts this experimental observation.

The situation changes in the presence of  $U = 16t$ , as shown in Fig. 3(b). Here, the dotted line represents our result for spin stiffness, Eq. (18); due to the zone-boundary softening effect discussed in Sec. II it is expected that for all carrier

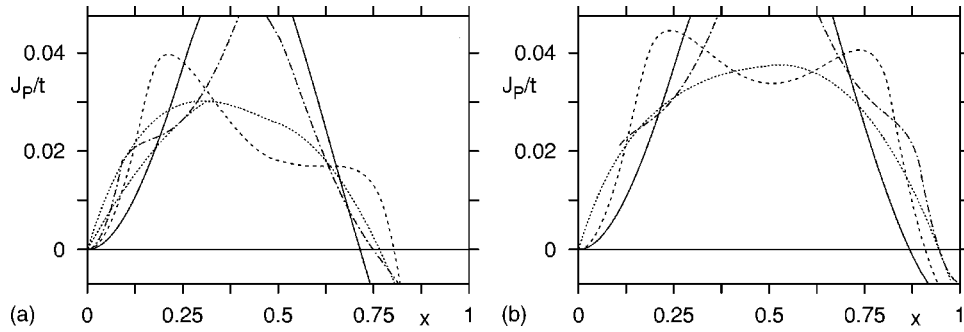


FIG. 3. Values of superexchange  $J$  corresponding to the instabilities of the ferromagnetic order at  $T=0$  in a 2D system with  $J_H/t=5$ ,  $U=0$  (a), and  $U/t=16$  (b). Dotted lines correspond to spin-wave instabilities, solid (dashed) lines—to the phase separation into G-type (A-type) antiferromagnetic and ferromagnetic phases, and the dashed-dotted line—to the phase separation into chain (see Fig. 4) and ferromagnetic phases.

concentrations, the spin-wave instability at  $\vec{p}=\{\pi, \pi\}$  corresponds to a slightly lower value of superexchange. The latter is not shown in Fig. 3(b) because our result for the magnon spectrum, Eq. (19), does not include the subleading (in  $t/J_S$ ) term and therefore should not be compared with other quantities plotted here. The Néel phase separation instability (solid line) is plotted using Eqs. (34), (A12), and (36). In order to improve accuracy for  $\mu(x) < -1$  (corresponding to  $x < 0.19$ ), we solved the full system of mean-field equations for the A-type phase. Nevertheless, we note that Eq. (40) yields accurate results in the region where the phase separation into ferromagnetic and A-type antiferromagnetic phases is possible.

We see that for  $U/t=16$  and  $J/t=0.015$  ( $J/t=0.02$ ), the region where ferromagnetic phase is unstable is shifted to  $1-x < 0.21$  ( $1-x < 0.23$ ), so that a *substantial stability region is now left for the ferromagnetic phase at  $x > 0.5$ , in agreement with experimental results*. Admittedly, the presence of broad stability region of ferromagnetic phase at  $x < 0.5$  is at variance with experiments and indicates a deficiency of either our variational procedure (i.e., our choice of possible phases is too narrow), or our simplified model, Eq. (1).<sup>56</sup> Indeed, in the 3D case the experimental data<sup>10,57</sup> show that the phase diagrams for different perovskite compounds differ in the electron-doped ( $x < 0.5$ ) region, suggesting the sensitivity to details of crystalline surrounding and perhaps the importance of orbital structure.

The inclusion of Hubbard interaction in principle could have brought about new charge-ordered antiferromagnetic (or ferrimagnetic) phases, which would not occur at  $U=0$ . While we tried to look into this possibility, we could not identify any such phases that would be stable within the experimentally relevant region of parameter values. This difficulty was encountered also by other workers in the field,<sup>4</sup> who could stabilize charge ordering only upon including a large intersite Coulomb repulsion.

It is however worth mentioning that some of the more complicated phases which are relevant for phase separation at  $U=0$  do show charge ordering owing to inequivalence of different lattice sites. This is exemplified by the *chain phase*,<sup>18</sup> shown schematically in Fig. 4. In Fig. 3, the critical value of superexchange, corresponding to phase separation into ferromagnetic and chain phases, is shown by the dashed-

dotted line; for the  $U=0$  case it was calculated exactly, whereas for  $U=16t$  we used the large Stoner bandsplitting expansion similar to the one described above for the A-antiferromagnetic phase. We see that when  $U$  is included, the phase separation into ferromagnetic and chain phases in the hole-doped region,  $x > 0.5$ , becomes impossible. This is in line with the general expectation that *Hubbard repulsion disfavors charge ordering at  $x > 0.5$* , when there is less space between electrons.

The present mean-field treatment allowed us to arrive at important conclusions regarding the effects of Hubbard repulsion on the possible instabilities of the homogeneous ferromagnetic phase. Nevertheless, we stress that the full zero-temperature phase diagrams for the model (1) both in the 2D and in a much more cumbersome 3D case are still lacking, and should only come from numerical experiments. This is a challenging problem, as some of the phases involved can be expected to have relatively large unit cells.

## V. CARRIER DENSITY OF STATES NEAR THE FERMI LEVEL

While the physical nature of carrier transport and magnetotransport in the CMR compounds near the Curie temperature remains largely unknown, it may be possible to single out an equilibrium property which is most closely related to

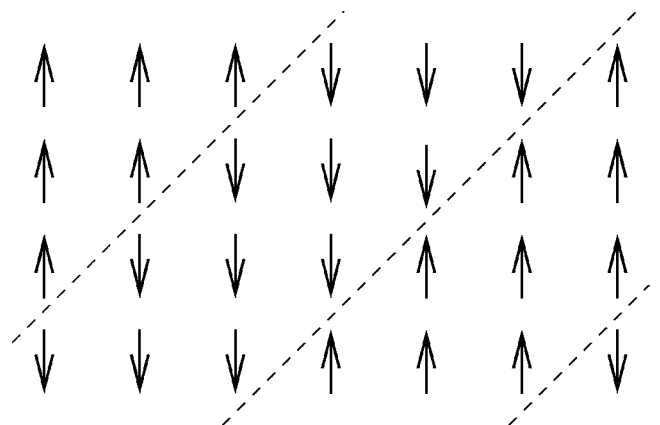


FIG. 4. Spin ordering in the chain phase.

the CMR phenomenon. It appears that such a property is a broad *depletion of carrier density of states near the Fermi level* as observed in photoemission/absorption in the CMR manganates.<sup>25</sup> This decrease of the density of states, visible already deep in the ferromagnetic phase, becomes progressively more pronounced as the temperature approaches  $T_C$ , around which there is no spectral weight left at the Fermi level within the accuracy of the experiments. These results were subsequently confirmed by the tunneling measurements;<sup>26</sup> it was suggested that the hard gap opening at  $T \approx T_C$  is responsible for the peak of the resistivity. The relevance of these gap or pseudogap phenomena for transport is underlined by the fact<sup>26</sup> that the “transport gap” seen in the activated temperature dependence of resistivity at  $T > T_C$  is roughly of the same order of magnitude (tenths of eV) as the width of the density of states depletion. Furthermore, it seems possible that in the case of the nonmanganate lightly doped or nondegenerate magnetic semiconductors, the well-known giant red shift of the optical absorption edge<sup>58</sup> (with optical gap decreasing as the temperature is lowered through  $T_C$ ; see the discussion in Ref. 2) may act as a counterpart of the temperature-dependent pseudogap observed in the manganates.

For the case of the CMR manganates, high-resolution tunneling measurements have recently been extended<sup>24</sup> down to liquid helium temperatures, revealing a noticeable, albeit narrow, depletion of the density of states near the Fermi level at  $T = 4.2$  K. Although the conclusive evidence is still lacking, it is most reasonable to expect that it is this feature which with increasing temperature evolves into the broad pseudogap observed near  $T = T_C$ . It is therefore important that a proper description of the low-temperature ferromagnetic state of the CMR compounds should include this anomaly.

Within the mean-field picture advanced in the present paper, at low temperatures and within the relevant doping range of  $1 - x \approx 0.3$ , the system is assumed to be in a homogeneous, half-metallic ferromagnetic state; deviations from ferromagnetic ordering (spin waves) freeze out at  $T \ll T_C$ . The resistivity of the sample is then determined by impurity scattering, and it is only a combination of the latter with the usual Coulomb repulsion (including the long-range component), which could result in any density of states feature near the Fermi level. Indeed, it is known from the work of Altshuler and Aronov<sup>59,60</sup> that electron-electron interactions in a diffusive conductor generate an anomaly in the tunnelling density of states, centered on the Fermi energy. We note that since the magnitude of effective interaction  $V_{eff}(T)$  in the manganates is much smaller than the corresponding (nearest-neighbor) term  $V_{nn}$  in the Coulomb repulsion (see Sec. III), the effects of  $V_{eff}(T)$  on the density of states can be omitted altogether.

We use the standard expression for the change in the density of states near the Fermi level,<sup>59,60</sup>

$$\delta\nu = \frac{1}{\sqrt{2}\pi^2} \cdot \frac{|\epsilon - \mu|^{1/2}}{(\hbar D_e)^{3/2}}, \quad (41)$$

where the overall pre-factor has been multiplied by two in order to account for half-metallicity of the system.<sup>61</sup> Assum-

ing  $t \sim 0.5$  eV and using the values  $\rho \sim 161 \mu\Omega$  cm for the resistivity of  $\text{La}_{0.7}\text{Ca}_{0.3}\text{MnO}_3$ <sup>24</sup> and  $a \sim 4$  Å for intersite distance, we estimate the diffusion constant  $D_e$  as  $D_e \sim [\rho e^2 \nu(\epsilon_F)]^{-1} \sim 6a^3 t / (\rho e^2) \sim 7$  cm<sup>2</sup>/s. The resulting estimate,

$$\frac{\delta\nu(\epsilon)}{\nu} \sim 0.03 \sqrt{\frac{|\epsilon - \mu|}{t}}, \quad (42)$$

is an order of magnitude smaller than the experimental results of Ref. 24, which show a 15% change in  $\delta\nu/\nu$  for  $|\epsilon - \mu| \sim 0.075$  eV. Furthermore, based on Eq. (41) one expects that the relative change in the density of states for  $\text{La}_{0.75}\text{Sr}_{0.25}\text{MnO}_3$  (characterized by smaller values of resistivity and by a larger bandwidth) should be about 10 times less than in the case of  $\text{La}_{0.7}\text{Ca}_{0.3}\text{MnO}_3$ , whereas experimentally the two curves differ by a factor of the order of 2. In addition, the experiments<sup>24</sup> yield  $\delta\nu/\nu \propto (\epsilon - \mu)^2$  within a relatively broad energy range of  $|\epsilon - \mu| < 0.02$  eV; this is in contrast with the standard theory,<sup>59,60</sup> which predicts a crossover to the square root law [cf. Eq. (41)] at  $|\epsilon - \mu| \sim T$ . Thus, we find that *the Altshuler-Aronov mechanism cannot possibly account for the Fermi-level density of states depletion in the CMR manganates* even at low temperatures.

We therefore conclude that the low-temperature ferromagnetic state of the CMR manganates is characterized by strong electron correlation effects. Since these are certainly not captured within the present mean-field approach this does not necessarily signify the deficiency of our simplified model, Eq. (1). While we plan to investigate this question in more detail in the future, we emphasize that our conclusion on the *correlated nature of the low-temperature ferromagnetic phase* of the CMR manganates is likely to be model-independent. In other words, an adequate generic model of the manganates, whether or not it involves orbital, lattice, etc. degrees of freedom, must necessarily take proper non-perturbative account of electron-electron interactions.

## VI. CONCLUSION

In the present paper, we were concerned with the effects of the strong on-site Coulomb repulsion which is present in the CMR compounds but often overlooked in the theoretical treatments. By treating the model within the mean-field approach, we were able to resolve some apparent discrepancies between the generically observed low-temperature properties of these compounds and theoretical results for the (noninteracting) double exchange model at the appropriate values of Hund’s rule coupling strength. These properties include the doping dependence of spin stiffness, and the “zone-boundary softening” of magnon spectrum (Sec. II) which has attracted much attention from both theorists and experimentalists. The underlying physical mechanisms are two-fold and include both the interaction-induced increase in the effective band splitting (Sec. I) and the correlated physics of the strongly interacting Hubbard carriers (Sec. III). In addition, we showed that a novel, magnon-mediated effective electron-electron interaction arises in these systems at finite temperatures (Sec. III). While for the CMR manganates the strength

of this interaction remains negligible, it is expected that it is much more important in the case of Eu-based magnetic semiconductors exhibiting CMR.

By considering the stability of the ferromagnetic state against phase separation, we were able to show (Sec. IV) that inclusion of the Hubbard repulsion alleviates another disagreement between the theory and experiment, resulting in a sizable stability region of the ferromagnetic state above half electron filling,  $x > 0.5$ . Regarding the phase diagram, the question of identification of the relevant phases and finding the precise domain of the ferromagnetic phase (especially in the electron-doped region,  $x < 0.5$ ) remains open and calls for further theoretical investigations, in particular numerical ones. At the same time we note that the underlying physics consists in a competition between many phases with very close values of thermodynamic potential, and the outcome is guaranteed to be strongly dependent on the details of band structure, lattice/orbital properties and interactions in a particular compound. Therefore, while understanding the details and implications of phase separation in the CMR compounds (including both thermodynamic and transport properties) presents a broad and fascinating problem, it is not obvious that these details are directly related to the generic features of the CMR phenomenon itself.

The satisfactory results of our mean-field approach, as sketched above, all have to do with the integral quantities, involving summation over the entire Fermi sea. It is precisely this effective averaging that makes our Hartree-Fock decoupling scheme a relatively reliable tool in this case. The situation changes drastically when this approach is used to address other issues, such as the behavior of the carrier density of states near the Fermi level (Sec. V). In this case, the usage of the Hartree-Fock approximation (which yields the effective Stoner band splitting  $J_S$  much larger than the Fermi energy, leading to an assumption that the system is half-metallic with no minority-spin carriers) is the probable cause of our inability to reproduce the experimentally measured<sup>24</sup> depletion of the density of states. Assuming that the results reported in Ref. 24 are sufficiently generic, this failure may have far-reaching conceptual consequences.

As mentioned in Sec. V, it is expected that the low-temperature depletion of the density of states at the Fermi level is a temperature-dependent feature, which with increasing temperature evolves into the pseudogap; this temperature dependence is in turn expected to crucially affect transport properties of the system both near  $T_C$  and at low temperatures. The failure to recover the low- $T$  Fermi-level feature in the density of states within a theoretical treatment based on the picture of a half-metallic homogeneous ferromagnetic phase (Sec. V) should lead to *questioning the experimental relevance of the many available calculations of the low-temperature resistivity in double exchange ferromagnets*, which are based on similar assumptions.

On the other hand, one should not overlook the evidence, coming both from band structure calculations<sup>14</sup> and the experimental observations,<sup>62</sup> which points to the *presence of carriers in the minority spin subband* in the CMR manganates even at low temperatures. Theoretically, this may be possible due to relatively small values of Hund's rule coupling; the spin-down (minority) electrons,<sup>63</sup> if present, will

form polaron-like localized states, accompanied by a reduction in the spin-up electron density within the area of the polaron (this reduction will in turn reduce the Coulomb/Hubbard interaction energy). These localized spin-down carriers will clearly lead to an enhanced spin-up electron scattering and will also affect the density of states at the Fermi level.<sup>64</sup> As explained in the Introduction, these correlated effects are beyond the mean-field approach used in the present paper; in our view, this scenario definitely merits further attention, especially as there is now some recognition<sup>65</sup> that other avenues of theoretical investigation of the CMR and related phenomena may have proved unpromising.

On the experimental side, we suggest that some key measurements still have to be performed in order to clarify the issues under discussion here. These fall into three categories.

(i) Detailed investigations of the energy dependence of the density of states as a function of temperature and magnetic field. This includes tunneling and optical measurements for various chemical composition and doping levels, within the entire temperature range, and would help to clarify the relationship between the low-temperature density of state depletion of the Fermi level<sup>24</sup> and the pseudogap observed in the near-critical region,<sup>25,26</sup> as well as confirm the relevance of these phenomena for transport and magnetotransport.

(ii) A systematic investigation of the interplay between pseudogap and other phenomena, in particular those related to the unusual spin correlations found in the CMR manganates, such as the central peak observed in the inelastic neutron scattering<sup>66</sup> and critical behavior of spin-stiffness.<sup>67</sup> In particular, it can be expected that understanding the nature of spin dynamics at elevated temperatures would shed light on the structure of electron states involved in the pseudogap formation. The relationship between pseudogap and phase separation should be clarified as well.

(iii) Lastly, what appears an important theoretical and experimental problem is to identify the "common denominator" between the structure and properties of the CMR manganates<sup>1</sup> and those of the CMR magnetic semiconductors (Eu-based) and spinels.<sup>2</sup> Understanding what these CMR compounds have in common may be of much help in constructing a minimal theoretical model for the CMR compounds. In connection to this, we recall that the familiar argument concerning the relative unimportance of  $U$  in systems with low carrier densities rests upon an assumption that carrier distribution throughout the sample is uniform on the microscopic scale. The latter is not expected to be true, both for the CMR manganates and for ferromagnetic semiconductors at elevated temperatures,  $T \lesssim T_C$ . It is therefore possible that the effects of  $U$ , discussed in this paper, are important in both systems.

## ACKNOWLEDGMENTS

I am indebted to J. T. Chalker for the many detailed discussions which provided me with his insight and counsel throughout all stages of work on the present article. I also take pleasure in thanking A. M. Finkelstein, K. A. Kikoin, J. W. Lynn, and S. Satpathy for valuable discussions. This work was supported by EPSRC Grant No. GR/M0442, by the ISF

of the Israeli Academy, by the EC RTN Spintronics, and by the Israeli Ministry of Absorption.

### APPENDIX: MEAN-FIELD EQUATIONS FOR THE $G$ -TYPE ANTIFERROMAGNETIC PHASE AT $T=0$

Here we outline the necessary details of the Hartree mean-field scheme, as applied in Sec. IV to the  $G$ -antiferromagnetic phase. Throughout this appendix, we use units in which the hopping constant,  $t$ , is equal to unity. Eq. (30) is diagonalized by

$$d_{\vec{k}\uparrow} = \frac{\epsilon_{\vec{k}}}{\sqrt{2\Omega_{\vec{k}}^2 - J_S^{(G)}\Omega_{\vec{k}}}} f_{\vec{k}\uparrow} + \frac{\epsilon_{\vec{k}}}{\sqrt{2\Omega_{\vec{k}}^2 + J_S^{(G)}\Omega_{\vec{k}}}} f_{\vec{k}\downarrow},$$

$$d_{\vec{k}\downarrow} = \frac{\frac{1}{2}J_S^{(G)} - \Omega_{\vec{k}}}{\sqrt{2\Omega_{\vec{k}}^2 - J_S^{(G)}\Omega_{\vec{k}}}} f_{\vec{k}\uparrow} + \frac{\frac{1}{2}J_S^{(G)} + \Omega_{\vec{k}}}{\sqrt{2\Omega_{\vec{k}}^2 + J_S^{(G)}\Omega_{\vec{k}}}} f_{\vec{k}\downarrow}, \quad (\text{A1})$$

with  $\Omega_{\vec{k}}^2 = \frac{1}{4}(J_S^{(G)})^2 + \epsilon_{\vec{k}}^2$ . Assuming that the system is still half-metallic, i.e., that the chemical potential lies below the bottom of the spin-down *antiferromagnetic* band [cf. Eq. (32)], we find

$$x_{\uparrow,\downarrow} = \frac{1}{2}x_G \pm \frac{1}{2}I, \quad I = \frac{1}{2N}J_S^{(G)} \sum_{\vec{k}} \frac{n_{\vec{k}}^{(G)}}{\Omega_{\vec{k}}}, \quad (\text{A2})$$

where  $n_{\vec{k}}^{(G)} \equiv \langle f_{\vec{k}\uparrow}^\dagger f_{\vec{k}\uparrow} \rangle$  is the appropriate Fermi distribution function. Together with Eqs. (32) and (33), Eq. (A2) forms a closed system of mean-field equations for a homogeneous  $G$ -antiferromagnetic phase at fixed  $x_G$ .

We note that the Fermi surface in a partially-filled spin-up band has two sheets, corresponding to different signs of  $\epsilon_{\vec{k}}$ . Thus, the quantity

$$\langle d_{i\uparrow}^\dagger d_{i\downarrow} \rangle = -\frac{1}{2N} \sum_{\vec{k}} \frac{\epsilon_{\vec{k}} n_{\vec{k}}^{(G)}}{\Omega_{\vec{k}}}$$

is always equal to zero, showing the consistency of mean-field decoupling used in Eq. (30).

When the carrier density in the ferromagnetic phase becomes sufficiently large for the inequality (34) to be violated, there arises a nonzero carrier density,  $x_G = x_\downarrow + x_\uparrow$  in the Néel phase. This in turn leads to an increase of quantities  $\delta$  and  $J_S^{(G)}$  in Eq. (32), resulting in the upward shift and narrowing of the antiferromagnetic band. This effect is more pronounced when the value of  $U$  is sufficiently large, in which case the energy difference between chemical potential and the bottom of  $G$ -antiferromagnetic band,

$$\zeta = \mu(x) - \frac{1}{2}J_H - \delta + \sqrt{\frac{1}{4}(J_S^{(G)})^2 + d^2}, \quad (\text{A3})$$

and the band-filling,

$$x_G = \begin{cases} \frac{(2\zeta)^{3/2}}{3^{5/2}\pi^2} \left[ \frac{1}{4}(J_S^{(G)})^2 + 9 \right]^{3/4} & \text{in three dimensions,} \\ \frac{\zeta}{2\pi} \sqrt{\frac{1}{4}(J_S^{(G)})^2 + 4} & \text{in two dimensions,} \end{cases} \quad (\text{A4})$$

remain small within an extended range of values of  $x$ . In this large- $U$  limit, it is possible to solve the mean-field equations analytically.

When the band filling is small,  $x_G \ll 1$ , Eqs. (A2) and (33) yield

$$J_S^{(G)} = J_H + UJ_S^{(G)} \frac{x_G}{\sqrt{(J_S^{(G)})^2 + 4d^2}}, \quad (\text{A5})$$

or

$$J_S^{(G)} = \frac{J_H}{1 - U\xi/2}, \quad \xi \equiv \frac{2x_G}{\sqrt{(J_S^{(G)})^2 + 4d^2}}. \quad (\text{A6})$$

Substituting this into Eq. (A3) [and also using Eq. (33) for  $\delta$ ], we obtain

$$\zeta + \frac{1}{2}J_H - \mu(x) = \sqrt{\frac{1}{4}J_H^2 + d^2 \left(1 - \frac{1}{2}U\xi\right)^2}. \quad (\text{A7})$$

We are interested in the large- $U$  situation when  $\zeta$  is small and can be omitted on the lhs [see below, Eq. (A13)], in which case we find, to leading order,

$$\xi \approx \frac{2}{U} \left\{ 1 - \frac{1}{d} \sqrt{\mu(x)[\mu(x) - J_H]} \right\}. \quad (\text{A8})$$

With the help of Eqs. (A6) this in turn yields

$$J_H^{(G)} = dJ_H / \sqrt{\mu(x)[\mu(x) - J_H]}. \quad (\text{A9})$$

While at  $\mu(x) = \mu_0$ , Eq. (A9) yields  $J_S^{(G)} = J_H$ , with a further increase of  $x$  [and hence  $\mu(x)$ ] towards the quarter-filling,  $\mu(x) = 0$ , the value of  $J_S^{(G)}$  increases, and the bandwidth [of the order of  $d^2/(J_S^{(G)})^2$ , see Eq. (32)] decreases, with the effect that the bottom of spin-up band in the  $G$ -antiferromagnetic phase remains pinned immediately below the chemical potential  $\mu(x) - \frac{1}{2}J_H$ . As a result, band-filling in the antiferromagnet,

$$x_G = \frac{2}{U} \left\{ \frac{d}{\sqrt{\mu(x)[\mu(x) - J_H]}} - 1 \right\} \cdot \left\{ \frac{1}{2}J_H - \mu(x) \right\}, \quad (\text{A10})$$

remains small as long as  $|\mu(x)| \gg J_H/U^2$ . When the latter inequality is violated, Eqs. (A9) and (A10) become invalid. Using Eqs. (31), (32), and (A3), we write for the thermodynamic potential in the case of small  $x_G$ ,

$$\Omega_G = -Ux_\uparrow x_\downarrow - dJ + \frac{1}{N} \sum_{\vec{k}} n_{\vec{k}}^{(G)} \times \left\{ \sqrt{\frac{1}{4}(J_S^{(G)})^2 + d^2} - \sqrt{\frac{1}{4}(J_S^{(G)})^2 + \epsilon_{\vec{k}}^2 - \zeta} \right\}. \quad (\text{A11})$$

The sum on the rhs [which can be evaluated using the small- $k$  expansion and Eq. (A4)] is found to be of the order of  $x_G \zeta$  and can be omitted. Equations (A2) and (A10) then yield the final expression,

$$\Omega_G = -\frac{1}{U} \{d - \sqrt{\mu(x)[\mu(x) - J_H]}\}^2 - dJ. \quad (\text{A12})$$

It is easy to see that our neglecting the first term on the lhs of Eq. (A7) is appropriate as long as

$$\zeta \frac{J_H - 2\mu(x)}{d\sqrt{\mu(x)[\mu(x) - J_H]}} \ll 1 - \frac{1}{d} \sqrt{\mu(x)[\mu(x) - J_H]}. \quad (\text{A13})$$

At small absolute values of  $\mu(x) < 0$ , this is satisfied as long as  $x_G \sim J_H^{1/2} |\mu|^{-1/2} / U$  is small [see Eqs. (A10) and (A4)]. On the other hand, when  $\mu(x)$  is close to  $\mu_0$  (when Eq. (A10) yields  $x_G \approx [\mu(x) - \mu_0](J_H^2 + 4d^2)/(Ud)$ ), Eq. (A13) takes form  $U \gg \pi(J_H^2 + 16)^{1/2}$  in two dimensions and  $U[\mu(x) - \mu_0]^{1/2} \gg \pi^2(\frac{1}{4}J_H^2 + 9)^{1/4}$  in three dimensions.<sup>68</sup> Since the actual value of  $U/t$  for the CMR manganates is about 16, our results in the latter region can be viewed as an order of magnitude estimate only.

As the value of  $x$  is increased towards half-filling, and the chemical potential reaches small (negative) values of  $\mu(x) \gtrsim -J_H/U^2$ , the value of  $x_G$  starts increasing rapidly. The spin-up  $G$ -antiferromagnetic band is filled,  $x_G = 1$ , for  $\mu(x) > dU/[2(J_H + U)^2]$  [cf. Eq. (32)]. In principle, the mean-field equations can also be analyzed within this narrow area near  $\mu(x) = 0$ , assuming that  $J_H + Ux_G$  is large.

\*Present address: Racah Institute of Physics, the Hebrew University, Jerusalem 91904, Israel. Electronic address: golosov@phys.huji.ac.il

<sup>1</sup> *Colossal Magnetoresistive Oxides*, edited by Y. Tokura (Gordon and Breach, New York, 2000), and references therein.

<sup>2</sup> E. L. Nagaev, *Colossal Magnetoresistance and Phase Separation in Magnetic Semiconductors* (Imperial College Press, London, 2002), and references therein.

<sup>3</sup> P. W. Anderson and H. Hasegawa, *Phys. Rev.* **100**, 675 (1955).

<sup>4</sup> S. K. Mishra, R. Pandit, and S. Satpathy, *J. Phys.: Condens. Matter* **11**, 8561 (1999).

<sup>5</sup> J. E. Medvedeva, V. I. Anisimov, O. N. Mryasov, and A. J. Freeman, *J. Phys.: Condens. Matter* **14**, 4533 (2002); J. E. Medvedeva, V. I. Anisimov, M. A. Korotin, O. N. Mryasov, and A. J. Freeman, *Magn. Mater.* **237**, 47 (2001).

<sup>6</sup> M. J. Rozenberg, *Eur. Phys. J. B* **2**, 457 (1998); V. Ferrari, M. J. Rozenberg, and R. Weht, *Mod. Phys. Lett. B* **15**, 1031 (2001); K. Held and D. Vollhardt, *Phys. Rev. Lett.* **84**, 5168 (2000); R. Maezono and N. Nagaosa, *Phys. Rev. B* **67**, 064413 (2003), and references therein.

<sup>7</sup> J. Kieinert, C. Santos, and W. Nolting, *Phys. Status Solidi B* **236**, 515 (2003).

<sup>8</sup> S. Satpathy, Z. S. Popović, and F. R. Vukajlović, *Phys. Rev. Lett.* **76**, 960 (1996).

<sup>9</sup> P. Schiffer, A. P. Ramirez, W. Bao, and S.-W. Cheong, *Phys. Rev. Lett.* **75**, 3336 (1995).

<sup>10</sup> C. Martin, A. Maignan, M. Hervieu, and B. Raveau, *Phys. Rev. B* **60**, 12 191 (1999).

<sup>11</sup> J. F. Mitchell, C. D. Ling, J. E. Millburn, D. N. Argyriou, A. Berger, and M. Medarde, *J. Appl. Phys.* **89**, 6618 (2001).

<sup>12</sup> In particular, it has recently been established that the CMR phenomenon takes place also in  $\text{LaMnO}_3$  doped with tetravalent ions such as Ce. These systems involve a mixture of  $\text{Mn}^{3+}$  and  $\text{Mn}^{2+}$  ions, and their orbital structure is expected to differ from

that of conventional manganates, corresponding to a  $\text{Mn}^{3+} - \text{Mn}^{4+}$  mixture [see, e.g., C. Mitra, P. Raychaudhuri, K. Dörr, K.-H. Müller, L. Schultz, P. M. Oppeneer, and S. Wirth, *Phys. Rev. Lett.* **90**, 017202 (2003); S. W. Han, J.-S. Kang, K. H. Kim, J. D. Lee, J. H. Kim, S. C. Wi, C. Mitra, P. Raychaudhuri, S. Wirth, K. J. Kim, B. S. Kim, J. I. Jeong, S. K. Kwon, and B. I. Min, *Phys. Rev. B* **69**, 104406 (2004)].

<sup>13</sup> J.-H. Park, E. Vescovo, H.-J. Kim, C. Kwon, R. Ramesh, and T. Venkatesan, *Nature (London)* **392**, 794 (1998).

<sup>14</sup> We note that bandstructure calculations predict incomplete spin polarization. See W. E. Pickett and D. J. Singh, *J. Magn. Magn. Mater.* **172**, 237 (1997).

<sup>15</sup> D. I. Golosov, *Phys. Rev. B* **67**, 064404 (2003).

<sup>16</sup> Due to these, the spin-up band in the antiferromagnetic phases at finite  $J_H$  is not symmetric with respect to  $\epsilon^{\uparrow} = -J_H/2$  [see Eq. (32) with  $\delta = 0$ ,  $J_S^{(G)} = J_H$ ]. As the spins deviate from ferromagnetic ordering, the double-exchange band narrowing effect is then complemented by the downward shift of the center of gravity of the band.

<sup>17</sup> E. Dagotto, *Nanoscale Phase Separation and Colossal Magnetoresistance* (Springer-Verlag, Berlin, 2003), and references therein.

<sup>18</sup> D. I. Golosov, *J. Appl. Phys.* **91**, 7508 (2002).

<sup>19</sup> In making this generic observation, we are not concerned with (i) the vicinity of the quarter-filling,  $x = 1/2$ , (ii) the distinction between metallic and insulating ferromagnetic states, and (iii)  $c$ -axis magnetic ordering in the layered CMR compounds.

<sup>20</sup> This point of commensurate filling may prove singular from the viewpoint of lattice and orbital effects, which are not considered here.

<sup>21</sup> See, e.g., Eqs. (9) and (10) in Ref. 15.

<sup>22</sup> The observation that Coulomb repulsion can promote ferromagnetism is due to Heisenberg and Dirac [see, e.g., J. H. van Vleck, *The Theory of Electric and Magnetic Susceptibilities* (Oxford

- University Press, Oxford, 1932)].
- <sup>23</sup>For an upper energy bound, consider a variational state, in which the spin-down particle is localized at a certain site (single-particle energy  $J_H$ ), and all the spin-down electron states are perturbed in such a way that their wave functions vanish on this site (combined single-particle energy  $\sim \epsilon_F$  with no many-body contribution).
- <sup>24</sup>J. Mitra, A. K. Raychaudhuri, Ya. M. Mukovskii, and D. Shulyatev, Phys. Rev. B **68**, 134428 (2003).
- <sup>25</sup>D. S. Dessau, T. Saitoh, C.-H. Park, Z.-X. Shen, P. Villeda, N. Hamada, Y. Moritomo, and Y. Tokura, Phys. Rev. Lett. **81**, 192 (1998); D. S. Dessau and Z.-X. Shen, in Ref. 1, and references therein; Y.-D. Chuang, A. D. Gromko, D. S. Dessau, T. Kimura, and Y. Tokura, Science **292**, 1509 (2001).
- <sup>26</sup>A. Biswas, S. Elizabeth, A. K. Raychaudhuri, and H. L. Bhat, Phys. Rev. B **59**, 5368 (1999).
- <sup>27</sup>D. I. Golosov, Phys. Rev. Lett. **84**, 3974 (2000).
- <sup>28</sup>The change of  $N_{\vec{q}}$  due to the off-diagonal terms in  $\mathcal{H}'_2$  and  $\mathcal{H}'_{i2}$  is an effect of higher order in  $1/S$ .
- <sup>29</sup>E. L. Nagaev, Phys. Rev. B **58**, 827 (1998).
- <sup>30</sup>As a result of our choice of  $W_{\vec{k},\vec{p}}$ , Eq. (9), the leading-order (in  $\epsilon_F/J_S$ ) contribution to magnon self-energy is entirely contained in  $\mathcal{H}'_2$ , while other terms account for smaller corrections. The latter, when combined with a subleading (in  $\epsilon_F/J_S$ ) contribution from  $\mathcal{H}'_2$ , yield the last term in Eq. (18).
- <sup>31</sup>Even though the condition  $J_S \gg \epsilon_F$  is then violated at sufficiently large  $x$ , one can still use Eq. (18). This is a special property of the  $U=0$  case [cf. Ref. 15, Eq. (4)].
- <sup>32</sup>See, e.g., L. Vasiliiu-Doloc, J. W. Lynn, Y. M. Mukovskii, A. A. Arsenov, and D. A. Shulyatev, J. Appl. Phys. **83**, 7342 (1998); P. Dai, J. A. Fernandez-Baca, E. W. Plummer, Y. Tomioka, and Y. Tokura, Phys. Rev. B **64**, 224429 (2001); K. Hirota, S. Ishihara, H. Fujioka, M. Kubota, H. Yoshizawa, Y. Moritomo, Y. Endoh, and S. Maekawa, *ibid.* **65**, 064414 (2002).
- <sup>33</sup>For a review see, e.g., T. Dombre, Helv. Phys. Acta **63**, 261 (1990); P. Würth, G. Uhrig, and E. Müller-Hartmann, Ann. Phys. (N.Y.) **5**, 148 (1996).
- <sup>34</sup>P. Würth and E. Müller-Hartmann, Eur. Phys. J. B **5**, 403 (1998).
- <sup>35</sup>In the opposite case of  $J_H \gg Ux$ , the standard (Heisenberg-like) expression for spin wave energy in a double exchange ferromagnet with  $J_H \rightarrow \infty$  is recovered.
- <sup>36</sup>In reality, the saturation value of  $\omega_{\vec{q}}$  may be reduced (and may also acquire some momentum dependence) if the fully spin-polarized state of the Hubbard model becomes unstable (see the preceding paragraph).
- <sup>37</sup>We note that quantum-spin corrections (Ref. 27) and the subleading terms in the  $\epsilon_F/J_S$  expansion both have non-Heisenberg momentum dependence. These effects, however, are not included in Eq. (19).
- <sup>38</sup>See, e.g., I. V. Solovyev and K. Terakura, Phys. Rev. Lett. **82**, 2959 (1999); G. Khaliullin and R. Kilian, Phys. Rev. B **61**, 3494 (2000).
- <sup>39</sup>S.-J. Sun, W.-C. Lu, and H. Chou, Physica B **324**, 286 (2002).
- <sup>40</sup>See, e.g., J. W. Lynn, J. Supercond. **13**, 263 (2000), and references therein; H. Y. Hwang, P. Dai, S.-W. Cheong, G. Aeppli, D. A. Tennant, and H. A. Mook, Phys. Rev. Lett. **80**, 1316 (1998); H. Fujioka, M. Kubota, K. Hirota, H. Yoshizawa, Y. Moritomo, and Y. Endoh, J. Phys. Chem. Solids **60**, 1165 (1999); T. Chatterji, L. P. Regnault, and W. Schmidt, Phys. Rev. B **66**, 214408 (2002).
- <sup>41</sup>T. G. Perring, D. T. Adroja, G. Chaboussant, G. Aeppli, T. Kimura, and Y. Tokura, Phys. Rev. Lett. **87**, 217201 (2001).
- <sup>42</sup>D. I. Golosov, J. Appl. Phys. **87**, 5804 (2000).
- <sup>43</sup>In this case  $\epsilon_F/J_H$  is not small, and instead of Eq. (19) we have to use the full expression for the  $U=0$ , finite- $J_H$  case. See E. L. Nagaev, Fiz. Tverd. Tela (Leningrad) **11**, 2779 (1969) [Sov. Phys. Solid State **11**, 2249 (1970)]; N. Furukawa, J. Phys. Soc. Jpn. **65**, 1174 (1996); and Ref. 42.
- <sup>44</sup>This contribution is of the same order in both  $\epsilon_F/J_S$  and  $1/S$ , but is smaller than the first one when the bare interaction  $U$  is small.
- <sup>45</sup>Namely,  $4\Gamma_{12,43}^\dagger = \{[\text{Eq. (21)}] - [1 \leftrightarrow 2]\} - \{3 \leftrightarrow 4\}$ .
- <sup>46</sup>Our mean-field approach overestimates the retardation energy scale, which in reality may be reduced from  $J_S$  to  $J_H + \epsilon_F$  (cf. footnote 23), provided that the latter is smaller.
- <sup>47</sup>Here,  $\vec{M}$  is defined as a *classical* vector; therefore the quantity (24) vanishes at  $T \rightarrow 0$ .
- <sup>48</sup>Z. Popović and S. Satpathy, Phys. Rev. Lett. **88**, 197201 (2002).
- <sup>49</sup>M. Umehara, Phys. Rev. B **60**, 445 (1999).
- <sup>50</sup>P. G. Steeneken, L. H. Tjeng, I. Elfimov, G. A. Sawatzky, G. Ghiringhelli, N. B. Brookes, and D.-J. Huang, Phys. Rev. Lett. **88**, 047201 (2002).
- <sup>51</sup>This effect of a partial “decoupling” of the stiff spin-polarized Fermi sea from the local spins also yields a negative contribution to spin-stiffness, discussed in Sec. II.
- <sup>52</sup>For related experimental results, see, e.g., A. A. Samokhvalov, N. A. Viglin, B. A. Gizhevskii, T. I. Arbutova, and N. M. Chebotaev, Phys. Status Solidi B **148**, 361 (1988).
- <sup>53</sup>J. E. Hirsch, Phys. Rev. Lett. **54**, 1317 (1985).
- <sup>54</sup>P. B. Visscher, Phys. Rev. B **10**, 943 (1974).
- <sup>55</sup>In order to determine the actual spatial structure of phase-separated state, one has to take into account long-range interactions, not included in our model, Eq. (1); this will not be attempted here. See, e.g., Refs. 2 and 15.
- <sup>56</sup>This difficulty was noted and discussed in Ref. 4.
- <sup>57</sup>See, e.g., O. Chmaissem, B. Dabrowski, S. Kolesnik, J. Mais, J. D. Jorgensen, and S. Short, Phys. Rev. B **67**, 094431 (2003); M. Pissas and G. Kallias, *ibid.* **68**, 134414 (2003).
- <sup>58</sup>P. Wachter, CRC Crit. Rev. Solid State Sci. **3**, 189 (1972), and references therein; S. G. Ovchinnikov, Phase Transitions **36**, 15 (1991), and references therein.
- <sup>59</sup>B. L. Altshuler and A. G. Aronov, Zh. Eksp. Teor. Fiz. **77**, 2028 (1979) [Sov. Phys. JETP **50**, 968 (1979)].
- <sup>60</sup>For a review, see B. L. Altshuler and A. G. Aronov, in *Electron-Electron Interactions in Disordered Solids*, edited by A. L. Efros and M. Pollak (North-Holland, Amsterdam, 1985).
- <sup>61</sup>This is because in a half-metal, all pairs of electrons have parallel spins, thus contributing to the exchange term in the electron self energy.
- <sup>62</sup>B. Nadgorny, I. I. Mazin, M. Osofsky, R. J. Soulen, Jr., P. Broussard, R. M. Stroud, D. J. Singh, V. G. Harris, A. Arsenov, and Ya. Mukovskii, Phys. Rev. B **63**, 184433 (2001).
- <sup>63</sup>The minority electrons are expected to belong to the spin-down  $t_{2g}$  bands. These are likely to correspond to lower energies than the spin-down component of the  $e_g$  band, represented throughout the present paper by the operators  $c_{\vec{q}}^\dagger$ .
- <sup>64</sup>We note that possible relevance of the polarons for the density of state depletion has been discussed, although in a different context, already in Ref. 24.
- <sup>65</sup>B. Michaelis and A. J. Millis, Phys. Rev. B **68**, 115111 (2003).
- <sup>66</sup>J. W. Lynn, R. W. Erwin, J. A. Borchers, Q. Huang, A. Santoro, J.

- L. Peng, and Z. Y. Li, Phys. Rev. Lett. **76**, 4046 (1996); J. W. Lynn, J. Supercond. **13**, 263 (2000), and references therein.
- <sup>67</sup>J. A. Fernandez-Baca, P. Dai, H. Y. Hwang, C. Kloc, and S.-W. Cheong, Phys. Rev. Lett. **80**, 4012 (1998); P. Dai, J. A. Fernandez-Baca, E. W. Plummer, Y. Tomioka, and Y. Tokura, Phys. Rev. B **64**, 224429 (2001); J. A. Fernandez-Baca, P. Dai, H. Kawano-Furukawa, H. Yoshizawa, E. W. Plummer, S. Katano, Y. Tomioka, and Y. Tokura, *ibid.* **66**, 054434 (2002).
- <sup>68</sup>When the latter inequality is reversed in the immediate vicinity of  $\mu(x)=\mu_0$ , interaction effects become unimportant and the usual 3-dimensional behavior of  $x_G \propto [\mu(x)-\mu_0]^{3/2}$  [cf. Eq. (A4)] is restored.